

NEW TECHNIQUES FOR RELATING DYNAMICALLY CLOSE GALAXY PAIRS TO MERGER AND ACCRETION RATES : APPLICATION TO THE SSRS2 REDSHIFT SURVEY

D. R. PATTON^{1,2,3}, R. G. CARLBERG³, R. O. MARZKE⁴, C. J. PRITCHET¹, L. N. DA COSTA⁵, & P. S. PELLEGRINI⁶

Accepted for Publication in the Astrophysical Journal

ABSTRACT

The galaxy merger and accretion rates, and their evolution with time, provide important tests for models of galaxy formation and evolution. Close pairs of galaxies are the best available means of measuring redshift evolution in these quantities. In this study, we introduce two new pair statistics, which relate close pairs to the merger and accretion rates. We demonstrate the importance of correcting these (and other) pair statistics for selection effects related to sample depth and completeness. In particular, we highlight the severe bias that can result from the use of a flux-limited survey. The first statistic, denoted N_c , gives the number of companions per galaxy, within a specified range in absolute magnitude. N_c is directly related to the galaxy merger rate. The second statistic, called L_c , gives the total luminosity in companions, per galaxy. This quantity can be used to investigate the mass accretion rate. Both N_c and L_c are related to the galaxy correlation function ξ and luminosity function $\phi(M)$ in a straightforward manner. Both statistics have been designed with selection effects in mind. We outline techniques which account for various selection effects, and demonstrate the success of this approach using Monte Carlo simulations. If one assumes that clustering is independent of luminosity (which is appropriate for reasonable ranges in luminosity), then these statistics may be applied to flux-limited surveys.

These techniques are applied to a sample of 5426 galaxies in the SSRS2 redshift survey. This is the first large, well-defined low- z survey to be used for pair statistics. Using close ($5 h^{-1} \text{ kpc} \leq r_p \leq 20 h^{-1} \text{ kpc}$) dynamical ($\Delta v \leq 500 \text{ km/s}$) pairs, we find $N_c(-21 \leq M_B \leq -18) = 0.0226 \pm 0.0052$ and $L_c(-21 \leq M_B \leq -18) = 0.0216 \pm 0.0055 \times 10^{10} h^2 L_\odot$ at $z=0.015$. These are the first secure estimates of low-redshift pair statistics, and they will provide local benchmarks for ongoing and future pair studies. If N_c remains fixed with redshift, simple assumptions imply that $\sim 6.6\%$ of present day galaxies with $-21 \leq M_B \leq -18$ have undergone mergers since $z=1$. When applied to redshift surveys of more distant galaxies, these techniques will yield the first robust estimates of evolution in the galaxy merger and accretion rates.

1. INTRODUCTION

Studies of galaxy evolution have revealed surprisingly recent changes in galaxy populations. Comparisons of present day galaxies with those at moderate ($z \sim 0.5$) and high ($z \sim 3$) redshift have uncovered trends which are often dramatic, and may trace galaxies to the time at which they were first assembled into recognizable entities. These discoveries have shed new light on the formation of galaxies, and have provided clues as to the nature of their evolution. At $z < 1$, the picture that is emerging is one in which early type galaxies evolve slowly and passively, while late type galaxies become more numerous with increasing redshift (e.g., Lin et al. 1999). At higher redshifts, deep surveys such as the Hubble Deep Field (Williams et al. 1996) indicate an increase in the cosmic star formation rate out to $z \sim 2$ (e.g., Madau, Pozzetti, and Dickinson 1998).

While considerable progress has been made in the observational description of galaxy evolution, important ques-

tions remain regarding the physical processes driving this evolution. Mechanisms that have been postulated include galaxy-galaxy mergers, luminosity-dependent luminosity evolution, and the existence of a new population of galaxies that has faded by the present epoch (see reviews by Koo & Kron 1992 and Ellis 1997). In this study, we will investigate the relative importance of mergers in the evolution of field galaxies. Mergers transform the mass function of galaxies, marking a progression from small galaxies to larger ones. In addition, mergers can completely disrupt their constituent galaxies, changing gas-rich spiral galaxies into quiescent ellipticals (e.g., Toomre and Toomre 1972). During a collision, a merging system may also go through a dramatic transition, with the possible onset of triggered star formation and/or accretion onto a central black hole (see review by Barnes & Hernquist 1992).

It is clear that mergers do occur, even during the relatively quiet present epoch. However, the frequency of these events, and the distribution of masses involved, has yet to

¹Department of Physics and Astronomy, University of Victoria, PO Box 3055, Victoria, BC, V8W 3P6, Canada, patton, pritchet@uvastro.phys.uvic.ca

²Guest User, Canadian Astronomy Data Centre, which is operated by the Herzberg Institute of Astrophysics, National Research Council of Canada.

³Department of Astronomy, University of Toronto, 60 St. George Street, Toronto, ON, M5S 3H8, Canada, patton, carlberg@astro.utoronto.ca

⁴Observatories of the Carnegie Institute of Washington, 813 Santa Barbara St., Pasadena, CA 91101, USA, marzke@ociw.edu

⁵European Southern Observatory, Karl-Schwarzschild-Strasse 2, 85748 Garching bei Munchen, Germany, ldacosta@eso.org

⁶Observatório Nacional, Rua General José Cristino 77, 20921-030 São Cristóvão, Rio de Janeiro, Brazil, pssp@on.br

be accurately established. This is true at both low and high redshift. Furthermore, while a number of attempts have been made, a secure measurement of evolution in the galaxy merger rate remains elusive, and a comparable measure of the accretion rate has yet to be attempted.

In this study, we introduce a new approach for relating dynamically close galaxy pairs to merger and accretion rates. These new techniques yield robust measurements for disparate samples, thereby allowing meaningful comparisons of mergers at low and high redshift. In addition, these pair statistics can be adapted to a variety of redshift samples, and to studies of both major and minor mergers. We apply these techniques to a large sample of galaxies at low redshift (SSRS2), providing a much needed local benchmark for comparison with samples at higher redshift. In a forthcoming paper (Patton et al. 2000), we will apply these techniques to a large sample of galaxies at moderate redshift (CNOC2; $0.1 < z < 0.6$), yielding a secure estimate for the rate of evolution in the galaxy merger and accretion rates.

An overview of earlier pair studies, and a discussion of their limitations and shortcomings, are given in the next section. The SSRS2 data are described in § 3. Section 4 discusses the connection between close pairs and the merger and accretion rates, while § 5 introduces new statistics for relating these quantities. Section 6 describes how these statistics can be applied to flux-limited surveys in a robust manner. A pair classification experiment is presented in § 7, giving empirical justification for our close pair criteria. Pair statistics are then computed for the SSRS2 survey in § 8, and the implications are discussed in § 9. Conclusions are given in the final section. Throughout this paper, we use a Hubble constant of $H_0 = 100h$ km s⁻¹ Mpc⁻¹. We assume $h=1$ and $q_0=0.1$, unless stated otherwise.

2. BACKGROUND

Every estimate of evolution in the merger and/or accretion rate begins with the definition of a merger statistic. Ideally, this statistic should be independent of selection effects such as optical contamination due to unrelated foreground/background galaxies, redshift incompleteness, redshift-dependent changes in minimum luminosity resulting from flux limits, contamination due to non-merging systems, k -corrections, and luminosity evolution. In addition, it should be straightforward to relate the statistic to the global galaxy population, and to measurements on larger scales. The statistic should then be applied to large, well-defined samples from low to high redshift, yielding secure estimates of how the merger and/or accretion rates vary with redshift.

Within the past decade, there have been a number of attempts to estimate evolution in the galaxy merger rate using close pairs of galaxies (e.g., Zepf & Koo 1989, Burkey et al. 1994, Carlberg, Pritchet, & Infante 1994, Woods, Fahlman, & Richer 1995, Yee & Ellingson 1995, Patton et al. 1997, Le Fèvre et al. 1999). The statistic that has been most commonly employed is the traditional pair fraction, which gives the fraction of galaxies with suitably close physical companions. This statistic is assumed to be proportional to the galaxy merger rate. The local (low-redshift) pair fraction was estimated by Patton et al.

(1997), using a flux-limited ($B \leq 14.5$) sample of galaxies from the UGC catalog (Nilson 1973). Using pairs with projected physical separations of less than $20 h^{-1}$ kpc, they estimated the local pair fraction to be $4.3 \pm 0.4\%$. This result was shown to be consistent with the local pair fraction estimates of Carlberg et al. (1994) and Yee & Ellingson (1995), both of whom also used the UGC catalog. The pair fraction has been measured for samples of galaxies at moderate redshift ($z \sim 0.5$), yielding published estimates ranging from approximately 0% (Woods, Fahlman, & Richer 1995) to $34\% \pm 9\%$ (Burkey et al. 1994). Evolution in the galaxy merger rate is often parameterized as $(1+z)^m$. Close pair studies have yielded a wide variety of results, spanning the range $0 \lesssim m \lesssim 5$. There are several reasons for the large spread in results. First, different methods have been used to relate the pair fraction to the merger rate. In addition, some estimates have been found to suffer from biases due to optical contamination or redshift completeness. After taking all of these effects into account, Patton et al. (1997) demonstrated that most results are broadly consistent with their estimate of $m = 2.8 \pm 0.9$, made using the largest redshift sample (545 galaxies) to date.

While this convergence seems promising, all of these results have suffered from a number of very significant difficulties. The central (and most serious) problem has been the comparison between low and moderate redshift samples. Low- z samples have been poorly defined, due to a lack of suitable redshift surveys. In addition, the pair fraction depends on both the clustering and mean density of galaxies. The latter is very sensitive to the limiting absolute magnitude of galaxies, leading to severe redshift-dependent biases when using flux-limited galaxy samples. These biases have not been taken into account in the computation of pair fractions, or in the comparison between samples at different redshifts.

While these problems are the most serious, there are several other areas of concern. A lack of redshift information has meant dealing with optical contamination due to unrelated foreground and background galaxies. Moreover, while one can statistically correct for this contamination, it is still not possible to discern low velocity companions from those that are physically associated but unbound, unless additional redshift information is available. Finally, there is no direct connection between the pair fraction and the galaxy correlation function (CF) and luminosity function (LF), making the results more difficult to interpret.

To address these issues, we have developed a novel approach to measuring pair statistics. We will introduce new statistics that overcome many of the afflictions of the traditional pair fraction. We will then apply these statistics to a large, well-defined sample of galaxies at low redshift.

3. DATA

The Second Southern Sky Redshift Survey (da Costa et al. 1998; hereafter SSRS2) consists of 5426 galaxies with $m_B \leq 15.5$, in two regions spanning a total of 1.69 steradians in the southern celestial hemisphere. The first region, denoted SSRS2 South, has boundaries $-40^\circ \leq \delta \leq -2.5^\circ$ and $b_{II} \leq -40^\circ$. The second region, SSRS2 North, is a more recent addition, and is bounded by $\delta \leq 0^\circ$ and $b_{II} \geq 35^\circ$. Galaxies were selected primarily from the list

of non-stellar objects in the *Hubble Space Telescope* Guide Star Catalog, with positions accurate to $\sim 1''$ and photometry with an rms scatter of ~ 0.3 magnitudes (Alonso et al. 1993, Alonso et al. 1994). Steps were taken to ensure that single galaxies were not mistakenly identified as close pairs, due to the presence of dust lanes, etc. (da Costa et al. 1998). In addition, careful attention was paid to cases where a very close pair might be mistaken for a single galaxy. This was found to make a negligible contribution to the catalog as a whole ($< 0.1\%$ of galaxies are affected). The effect on the pairs analysis in this paper is further reduced by imposing a minimum pair separation of $5 h^{-1}$ kpc (see § 7).

The sample now includes redshifts for all galaxies brighter than $m_B \leq 15.5$. We correct all velocities to the local group barycenter using Equation 6 from Courteau and van den Bergh (1999). We restrict our analysis to the redshift range $0.005 \leq z \leq 0.05$. This eliminates nearby galaxies, for which recession velocities are dominated by peculiar velocities, giving poor distance estimates. We also avoid the sparsely sampled high redshift regime. This leaves us with a well-defined sample of 4852 galaxies.

4. THE GALAXY MERGER RATE AND ACCRETION RATE

4.1. Definitions

The primary goal of earlier close pair studies has been to determine how the galaxy merger rate evolves with redshift. The merger rate affects the mass function of galaxies, and may also be connected to the cosmic star formation rate. Before attempting to measure the merger rate, it is important to begin with a clear definition of a merger and a merger rate. Here, we refer to mergers between two galaxies which are both above some minimum mass or luminosity. If this minimum corresponds roughly to a typical bright galaxy (L_*), this criterion can be thought of as selecting so-called major mergers. We consider two merger rate definitions. First, it is of interest to determine the number of mergers that a typical galaxy will undergo per unit time. In this case, the relevant rate may be termed the galaxy merger rate (hereafter \mathcal{R}_{mg}). A related quantity is the total number of mergers taking place per unit time per unit co-moving volume. We will refer to this as the volume merger rate (hereafter $\mathcal{R}_{\text{mg}_V}$). Clearly, $\mathcal{R}_{\text{mg}_V} = n_0 \mathcal{R}_{\text{mg}}$, where n_0 is the co-moving number density of galaxies.

While both of these merger rates provide useful measures of galaxy interactions, they have their limitations. As one probes to faint luminosities, one will find an increasing number of faint companions; hence, the number of inferred mergers will increase in turn. For all realistic LFs, this statistic will become dominated by dwarf galaxies. In addition, it is of interest to determine how the mass of galaxies will change due to mergers. To address these issues, we will also investigate the rate at which mass is being accreted onto a typical galaxy. This quantity, the total mass accreted per galaxy per unit time, will be referred to as the galaxy accretion rate (hereafter \mathcal{R}_{ac}). This is related to the rate of mass accretion per unit co-moving volume ($\mathcal{R}_{\text{ac}_V}$) by $\mathcal{R}_{\text{ac}_V} = n_0 \mathcal{R}_{\text{ac}}$. The mass (or luminosity) dependence of the accretion rate means that it will be dominated by relatively massive (or luminous) galaxies, with dwarfs playing a very minor role unless the mass function is very steep.

4.2. Observable Quantities

In order to determine \mathcal{R}_{mg} observationally, one may begin by identifying systems which are destined to merge. By combining information about the number of these systems and the timescale on which they will undergo mergers, one can estimate an overall merger rate. Specifically, if one identifies N_m ongoing mergers per galaxy, and if the average merging timescale for these systems is T_{mg} , then $\mathcal{R}_{\text{mg}} = N_m/T_{\text{mg}}$. If the mass involved in these mergers (per galaxy) is M_m , then $\mathcal{R}_{\text{ac}} = M_m/T_{\text{mg}}$.

In practice, direct measurement of these quantities is a daunting task. It is difficult to determine if a given system will merge; furthermore, estimating the merger timescale for individual systems is challenging with the limited information generally available. However, if one simply wishes to determine how the merger rate is *changing* with redshift, then the task is more manageable. If one has the same definition of a merger in all samples under consideration, then it is reasonable to assume that the merger timescale is the same for these samples. In this case, we are left with the task of measuring quantities which are directly proportional to the number or mass of mergers per galaxy or per unit co-moving volume. If one wishes to consider luminosity instead of mass, the relation between mass and luminosity must either be the same at all epochs, or understood well enough to correct for the differences.

We have considered several quantities that fit this description. All involve the identification of close physical associations of galaxies. A “close companion” is defined as a neighbour which will merge within a relatively short period of time ($T_{\text{mg}} \ll t_H$), which allows an estimate of the instantaneous merger/accretion rate. If a galaxy is destined to undergo a merger in the very near future, it must have a companion close at hand. One might attempt to estimate the number of mergers taking place within a sample of galaxies. For example, a close pair of galaxies would be considered one merger, while a close triple would lead to two mergers, etc. Owing to the difficulty of determining with certainty which systems are undergoing mergers, we will not use this approach. One alternative is to estimate the number of galaxies with one or more close companions, otherwise known as the pair fraction. One drawback of this approach is that close triples or higher order N-tuples complicate the analysis, since they are related to higher orders of the correlation function. This also makes it difficult to correct for the flux-limited nature of most redshift surveys. As a result, we choose to steer clear of this method also.

In this study, we choose instead to use the *number and luminosity of close companions* per galaxy. The number of close companions per galaxy, hereafter N_c , is similar in nature to the pair fraction. In fact, they are identical in a volume-limited sample with no triples or higher order N-tuples. However, N_c will prove to be much more robust and versatile. We assume that N_c is directly proportional to the number of mergers per galaxy, such that $N_m = kN_c$ (k is a constant). This pairwise statistic is preferable to the number of mergers per galaxy or the fraction of galaxies in merging systems, in that it is related, in a direct and straightforward manner, to the galaxy two-point CF and the LF (see Section 5). We note that it is not necessary

that there be a one-to-one correspondence between companions and mergers, as long as the correspondence is the same, on average, in all samples under consideration.

Using this approach to estimate the number of mergers per galaxy, the merger rate is then given by $\mathcal{R}_{\text{mg}} = kN_c/T_{\text{mg}}$. The actual value of k depends on the merging systems under consideration. If one identifies a pure set of galaxy pairs, each definitely undergoing a merger, then each pair, consisting of 2 companions, would lead to one merger, giving $k=0.5$. For a pair sample which includes some triples and perhaps higher order N-tuples, $k < 0.5$. If the merging sample under investigation contains some systems which are not truly merging (for instance, close pairs with hyperbolic orbits), then k will also be reduced. While k clearly varies with the type of merging system used, the key is for k to be the same for all samples under consideration.

We take a similar approach with the accretion rate. We again use close companions, and in this case we simply add up the luminosity in companions, per galaxy (L_c). Defining the mean companion mass-to-light ratio as Υ , it follows that $M_m = \Upsilon L_c$ and $\mathcal{R}_{\text{ac}} = \Upsilon L_c/T_{\text{mg}}$. When comparing different samples, any significant differences in Υ must be accounted for.

4.3. A Simple Model of Mass Function Evolution Due to Mergers

In order to motivate further the need for merger rate measurements, and to set the stage for future work relating pair statistics to the mass and luminosity function, we develop a simple model which relates these important quantities. Suppose the galaxy mass function is given by $\phi(M, t)$. This function gives the number density of galaxies of mass M at time t , per unit mass. The model that follows can also be expressed in terms of luminosity or absolute magnitude, rather than mass.

We begin by assuming that all changes in the mass function are due to mergers. While this is clearly simplistic, this model will serve to demonstrate the effects that various merger rates can have on the mass function. In order to relate the mass function to the observable luminosity function, we further assume that mergers do not induce star formation. Again, this is clearly an oversimplification; however, this simple case will still provide a useful lower limit on the relative contribution of mergers to LF evolution. Finally, we assume that merging is a binary process.

Following Bahcall & Tremaine (1988), we consider how $\phi(M, t)$ evolves as the universe ages from time t to time $t+\Delta t$. Each merger will remove two galaxies from the mass function, and produce one new galaxy. Let $\Delta\phi(M, \Delta t)_{\text{out}}$ represent the decrease in the mass function due to galaxies removed by mergers, while $\Delta\phi(M, \Delta t)_{\text{in}}$ gives the increase due to the remnants produced by these mergers. Evolution in the mass function can then be given by

$$\phi(M, t + \Delta t) = \phi(M, t) - \Delta\phi(M, \Delta t)_{\text{out}} + \Delta\phi(M, \Delta t)_{\text{in}}. \quad (1)$$

We model this function by considering all galaxy pairs, along with an expression for the merging likelihood of each. Let $p(M, M', \Delta t)$ denote the probability that a galaxy of mass M will merge with a galaxy of mass M' in time interval Δt . In order to estimate $\Delta\phi(M, \Delta t)_{\text{out}}$, we need to

take all galaxies of mass M , and integrate over all companions, yielding

$$\Delta\phi(M, \Delta t)_{\text{out}} = \int_0^\infty \phi(M, t)\phi(M', t)p(M, M', \Delta t)[h^{-1}\text{Mpc}]^3 dM'. \quad (2)$$

We devise a comparable expression for $\Delta\phi(M, \Delta t)_{\text{in}}$ by integrating over all pairs with end-products of mass M . This is achieved by considering all pairs with component of mass $M - M'$ and M' , such that

$$\Delta\phi(M, \Delta t)_{\text{in}} = \int_0^\infty \phi(M - M', t)\phi(M', t) \times p(M - M', M', \Delta t)[h^{-1}\text{Mpc}]^3 dM'. \quad (3)$$

We can also express Equation 1 in terms of the pair statistics outlined in Section 4.2. If one considers close companions of mass $M' \leq \infty$ next to primary galaxies of mass M , the volume merger rate can be expressed as $\mathcal{R}_{\text{mg}_V}(M)$, yielding

$$\Delta\phi(M, \Delta t)_{\text{out}} = \mathcal{R}_{\text{mg}_V}(M)\Delta t. \quad (4)$$

Similarly, if one defines a merger remnant statistic, $\mathcal{R}_{\text{mr}_V}(M)$, to be the co-moving number density of merger remnants per unit time corresponding to these same mergers, then

$$\Delta\phi(M, \Delta t)_{\text{in}} = \mathcal{R}_{\text{mr}_V}(M)\Delta t. \quad (5)$$

Therefore, it is possible, in principle, to use pair statistics to measure the evolution in the mass or luminosity function due to mergers. However, current pair samples are too small to permit useful pair statistics for different mass combinations. In addition, present day observations of close pairs are not of sufficient detail to determine the proportion of pairs that will result in mergers (factor k in previous section). Moreover, timescale estimates for these mergers are not known with any degree of certainty. Hence, useful observations of mass function evolution due to mergers will have to wait for improved pair samples and detailed estimates of merger timescales.

5. A NEW APPROACH TO MEASURING PAIR STATISTICS

In this section, we outline the procedure for measuring the mean number (N_c) and luminosity (L_c) of close companions for a sample of galaxies with measured redshifts. We begin by defining these statistics in real space, demonstrating how they are related to the galaxy LF and CF. We then show how these statistics can be applied in redshift space.

5.1. Pair Statistics in Real Space

In this study, we will measure pair statistics for a complete low-redshift sample of galaxies (SSRS2). However, we wish to make these statistics applicable to a wide variety of redshift samples. We would also like this method to be useful for studies of minor mergers, where one is interested in faint companions around bright galaxies. Moreover, these techniques should be adaptable to redshift samples with varying degrees of completeness (that is,

with redshifts not necessarily available for every galaxy). Therefore, in the following analysis, we treat host galaxies and companions differently.

Consider a primary sample of N_1 host galaxies with absolute magnitudes $M \leq M_1$, lying in some volume V . Suppose this volume also contains a secondary sample of N_2 galaxies with $M \leq M_2$. In the general case, the primary and secondary samples may have galaxies in common. This includes the special case in which the two samples are identical. If $M_1 \approx M_2$, this will tend to probe major mergers. If M_2 is chosen to be significantly fainter than M_1 , this will allow for the study of minor mergers. We assume here that both samples are complete to the given absolute magnitude limits; in Section 6, we extend the analysis from volume-limited samples to those that are flux-limited.

We wish to determine the mean number and luminosity of companions (in the secondary sample) for galaxies in the primary sample. In real space, we define a close companion to be one that lies at a true physical separation of $r \leq r^{\max}$, where r^{\max} is some appropriate maximum physical separation. To compute the observed mean number (N_c) and luminosity (L_c) of companions, we simply add up the number (N_{c_i}) and luminosity (L_{c_i}) of companions for each of the N_1 galaxies in the primary sample, and then compute the mean. Therefore,

$$N_c(M \leq M_2) = \sum_{i=1}^{N_1} N_{c_i}/N_1 \quad (6)$$

and

$$L_c(M \leq M_2) = \sum_{i=1}^{N_1} L_{c_i}/N_1. \quad (7)$$

We can also estimate what these statistics should be, given detailed knowledge of the galaxy two-point CF ξ and the LF $\phi(M)$. This is necessary if one wishes to relate these pair statistics to measurements on larger scales. Consider a galaxy in the primary sample with absolute magnitude M_i at redshift z_i . We would first like to estimate the number and luminosity of companions lying in a shell at physical distance (*proper* co-ordinates) $r \leq r_{ij} \leq r + dr$ from this primary galaxy. To make this estimate, we need to know the mean density of galaxies (related to the LF), and the expected overdensity in the volume of interest (given by the CF). The mean physical number density of galaxies at redshift z_i in the secondary sample, with absolute magnitudes $M \leq M_j \leq M + dM$, is given by

$$n_2(z_i, M)dM = (1 + z_i)^3 \phi(M, z_i)dM, \quad (8)$$

where $\phi(M, z_i)$ is the differential galaxy LF, which specifies the *co-moving* number density of galaxies at redshift z_i , in units of $h^3 \text{Mpc}^{-3} \text{mag}^{-1}$. The actual density of objects in the region of interest is determined by multiplying the mean density by $(1+\xi)$, where ξ is the overdensity given by the two-point CF (Peebles 1980). In general, ξ depends on the pair separation r , the mean redshift z_i , the absolute magnitude of each galaxy (M_i, M_j), and the orbits involved, specified by components parallel (v_{\parallel}) and perpendicular (v_{\perp}) to the line of sight. It follows that the

mean number of companions with $M \leq M_j \leq M + dM$ and $r \leq r_{ij} \leq r + dr$ is given by

$$N_{c_i}(z_i, M_i, M, r, v_{\perp}, v_{\parallel})dMdr = n_2(z_i, M)dM[1 + \xi(r, z_i, M_i, M, v_{\perp}, v_{\parallel})]4\pi r^2 dr. \quad (9)$$

We must now integrate this expression for all companions with $M \leq M_2$ and $r \leq r^{\max}$. Integration over the LF yields

$$n_2(z_i, M \leq M_2) = (1 + z_i)^3 \int_{-\infty}^{M_2} \phi(M, z_i)dM. \quad (10)$$

Integration over the CF is non-trivial, because of the complex nature of $\xi(r, z_i, M_i, M, v_{\perp}, v_{\parallel})$. With redshift samples that are currently available, it is not possible to measure this dependence accurately for the systems of interest. Hence, we must make three important assumptions at this stage. First, we assume that ξ is independent of luminosity. Later in the paper, we demonstrate empirically that this is a reasonable assumption, provided one selects a sample with appropriate ranges in absolute magnitude (see Section 6.1). Secondly, we assume that the distribution of velocities is isotropic. If one averages over a reasonable number of pairs, this is bound to be true, and therefore ξ is independent of v_{\perp} and v_{\parallel} . Finally, we assume that the form of the CF, as measured on large scales, can be extrapolated to the small scales of interest here. This assumption applies only to the method of relating pairs to large scale measures, and not to the actual measurement of pair statistics.

It is now straightforward to integrate Equation 9. The mean number of companions with $M \leq M_2$ and $r \leq r^{\max}$ for a primary galaxy at redshift z_i is given by

$$N_{c_i}(z_i, M \leq M_2, r \leq r^{\max}) = n_2(z_i, M \leq M_2) \int_0^{r^{\max}} [1 + \xi(r, z_i)]4\pi r^2 dr. \quad (11)$$

We derive an analogous expression for the mean luminosity in companions. The integrated luminosity density is given by

$$j_2(z_i, M \leq M_2) = (1 + z_i)^3 \int_{-\infty}^{M_2} \phi(M, z_i)L(M)dM, \quad (12)$$

where

$$L(M) = 10^{-0.4(M-M_{\odot})}L_{\odot}. \quad (13)$$

Therefore,

$$L_{c_i}(z_i, M \leq M_2, r \leq r^{\max}) = j_2(z_i, M \leq M_2) \int_0^{r^{\max}} [1 + \xi(r, z_i)]4\pi r^2 dr. \quad (14)$$

Given measurements of the CF on large scales, it is then straightforward to integrate these equations to arrive at predicted values of N_{c_i} and L_{c_i} .

It is important to note that these statistics are directly dependent on M_2 , which affects the mean density of galaxies in the secondary sample. This is different from statistics such as the correlation function, which are independent of density. Hence, this serves as a reminder that we

must exercise caution when choosing our samples, to ensure that differences in the pair statistics (and hence in the merger and accretion rates) are not simply due to apparent density differences resulting from selection effects. In addition, note that the choice of M_1 has no density-related effects on N_c and L_c .

5.2. Dynamical Pairs in Redshift Space

While it is preferable to identify companions based on their true physical pair separation, this is clearly not feasible when dealing with data from redshift surveys. In the absence of independent distance measurements for each galaxy, one must resort to identifying companions in redshift space. In this section, we outline a straightforward approach for measuring our new pair statistics in redshift space. We then attempt to relate these statistics to their counterparts in real space.

For any given pair of galaxies in redshift space, one can compute two basic properties which describe the intrinsic pair separation: the projected physical separation (hereafter r_p) and the rest-frame relative velocity along the line of sight (hereafter Δv). For a pair of galaxies with redshifts z_i (primary galaxy) and z_j (secondary), with angular separation θ , these quantities are given by $r_p = \theta d_A(z_i)$ and $\Delta v = c|z_j - z_i|/(1 + z_i)$, where $d_A(z_i)$ is the angular diameter distance at redshift z_i . Note that r_p gives the projected separation at the redshift of the primary galaxy.

We define a close companion as one in which the separation (both projected and line-of-sight) is less than some appropriate separation, such that $r_p \leq r_p^{\max}$ and $\Delta v \leq \Delta v^{\max}$. The line-of-sight criterion depends on both the physical line-of-sight separation and the line-of-sight peculiar velocity of the companion. It is of course not possible to determine the relative contributions of these components without distance information. However, for the small companion separations we will be concerned with, the peculiar velocity component is likely to be dominant in most cases, as we will be dealing with a field sample of galaxies (the same would not be true in the high velocity environment of rich clusters). Hence, this criterion serves primarily to identify companions with low peculiar velocities. While this is fundamentally different from the pure separation criterion used in real space, it too will serve to identify companions with the highest likelihood of undergoing imminent mergers. Using this definition of a close companion, it is straightforward to compute N_c and L_c , using Equations 6 and 7. Thus, the complexities of redshift space do not greatly complicate the computation of these pair statistics.

As in real space, we wish to relate these statistics to measurements on larger scales, given reasonable assumptions about the LF and CF. The situation is more complicated in redshift space, and therefore involves additional assumptions. We stress, however, that these assumptions apply only to the method of relating pair statistics to large scale measures, and not to the measured pair statistics themselves. To outline an algorithm for generating these predictions, we follow the approach of the previous section. We begin by modifying Equations 11 and 14, integrating over the new pair volume defined in redshift space. In order to do this, we use the two dimensional correlation

function in redshift space, $\xi_2(r_p, r_v, z)$, giving

$$N_{c_i}(z_i, M \leq M_2, r_p \leq r_p^{\max}, |r_v| \leq r_v^{\max}) = n_2(z_i, M \leq M_2) \int_{-r_v^{\max}}^{r_v^{\max}} \int_0^{r_p^{\max}} [1 + \xi_2(r_p, r_v, z_i)] 2\pi r_p dr_p dr_v \quad (15)$$

and

$$L_{c_i}(z_i, M \leq M_2, r_p \leq r_p^{\max}, |r_v| \leq r_v^{\max}) = j_2(z_i, M \leq M_2) \int_{-r_v^{\max}}^{r_v^{\max}} \int_0^{r_p^{\max}} [1 + \xi_2(r_p, r_v, z_i)] 2\pi r_p dr_p dr_v. \quad (16)$$

The two dimensional correlation function is the convolution of the velocity distribution in the redshift direction, $F(v_z)$, with the spatial correlation function $\xi(r, z)$, given by

$$\xi_2(x_p, x_v, z) = \int_{-\infty}^{\infty} \xi(\sqrt{x_p^2 + y^2}, z) F(H(z)[y - x_v]) dy. \quad (17)$$

Here, $H(z)$ is the Hubble constant at redshift z , given by $H(z) = H_0(1 + z)\sqrt{1 + \Omega_0 z}$. We have ignored the effect of infall velocities, which must be taken into account at larger radii but is an acceptable approximation for small separations. If the form of the CF and LF are known, it is straightforward to integrate Equations 15 and 16, yielding predictions of N_c and L_c .

5.3. Physical Pairs in Redshift Space

It is not always possible to have precise redshifts for all galaxies of interest in a sample. A common scenario with redshift surveys is to have redshifts available for a subset of galaxies identified in a flux-limited photometric sample. The photometric sample used to select galaxies for follow-up spectroscopy probes to fainter apparent magnitudes than the spectroscopic sample. In addition, the spectroscopic sample may be incomplete, even at the bright end of the sample. In this section, we will describe the procedure for applying pair statistics to this class of samples.

Suppose the primary sample is defined as all galaxies in the spectroscopic sample with absolute magnitudes $M \leq M_1$. The secondary sample consists of all galaxies lying in the photometric sample, regardless of whether or not they have measured redshifts. Once again, there may be some overlap between the primary and secondary samples. We must now identify close pairs. For each primary-secondary pair, we can compute r_p in precisely the same manner as before (see previous section), since we need only the redshift of the primary galaxy and the angular separation of the pair. However, we are no longer able to compute the relative velocity along the line of sight, since this requires redshifts for both members of the pair. Thus, we do not have enough information to identify close dynamical pairs. However, it is still possible to determine, in a statistical manner, how many physically associated companions are present. This is done by comparing the number (or luminosity) of observed companions with the number (or luminosity) expected in a random distribution.

As stressed in Section 5.1, pair statistics depend on the minimum luminosity M_2 imposed on the secondary sample. While we are now unable to compute the actual luminosity for galaxies in the secondary sample, we must still

impose M_2 if the ensuing pair statistics are to be meaningful. To do this, we make use of the fact that all physical companions must lie at approximately the same redshift as the primary galaxy under consideration. Therefore, M_2 corresponds to a limiting *apparent* magnitude m_2 at redshift z_i , such that

$$m_2 = M_2(z_i) - 5 \log h + 25 + 5 \log d_L(z_i) + k(z_i), \quad (18)$$

where $d_L(z_i)$ is the luminosity distance at redshift z_i , and $k(z_i)$ is the k -correction.

To begin, one finds all observed close companions with $m \leq m_2(z_i)$, using only the r_p criterion. This results in the quantities N_c^D and L_c^D , where the “D” superscript denote companions found in the data sample. One must then estimate the number (N_c^R) and luminosity (L_c^R) of companions expected at random. The final pair statistics for close physical companions are then given by $N_c = N_c^D - N_c^R$ and $L_c = L_c^D - L_c^R$.

We will now describe how to predict these statistics using the known LF and CF. This is relatively straightforward, since the excess ξ given by the CF is determined by the relative proportions of real and random companions. The pair statistics are once again integrals over the two dimensional CF in redshift space, as specified by Equations 15 and 16. In the “ $1 + \xi$ ” term, the first part gives the random contribution, while the second gives the excess over random. Thus, these pair statistics give the true density of companions, rather than the “excess” density. This is intentional, since mergers will occur even in an uncorrelated, randomly distributed sample of galaxies. At the small separations of interest, usually less than 1% of the correlation length, the difference between the mean density and the mean overdensity is less than about 0.01% in real space. For practical measurements in redshift space, where $r_v = \Delta v H(z)^{-1}$ is of order the correlation length, the background contribution is substantially larger than real space, but still amounts to less than 1%. Thus, for the close pairs considered in this study, it is reasonable to ignore the contribution that random companions make to the sample of physical companions. That is, we take $1 + \xi \approx \xi$. This allows us to relate the predictions to the measured pair statistics set out above. In principle, Equations 15 and 16 can be integrated over the range $-\infty < r_v < \infty$ to obtain predictions of N_c and L_c .

5.4. Application to Volume-limited Monte Carlo Simulations

To illustrate the concepts introduced so far, and to emphasize how these statistics depend on M_2 , we apply these techniques to volume-limited Monte Carlo simulations, which mimic the global distribution of galaxies in the SSRS2 North and South catalogs. Using $q_0=0.5$, galaxies are distributed randomly within the co-moving volume enclosed by $0.005 \leq z \leq 0.05$ and the SSRS2 boundaries on the sky (see Section 3). All peculiar velocities are set to zero. To create a volume-limited sample, we impose a minimum luminosity of $M_B=-16$, and assign luminosities using the SSRS2 LF (Marzke et al. 1998), which has Schechter function parameters $M_* - 5 \log h = -19.43$, $\alpha = -1.12$, and $\phi_* = 0.0128 h^3 \text{Mpc}^{-3} \text{mag}^{-1}$. An arbitrarily large number of galaxies can be generated, which is of

great assistance when looking for small systematic effects. We produce 16000 galaxies in the South, and 8070 in the North; this gives the same density of galaxies in both regions.

Using these simulations, we compute N_c and L_c . As these galaxies are distributed randomly (as opposed to real galaxies which are clustered), close pairs are relatively rare. To ensure a reasonable yield of pairs, we use a pair definition of $r_p^{\text{max}}=1 h^{-1} \text{Mpc}$ and $\Delta v^{\text{max}}=1000 \text{km/s}$. We note that there are no peculiar velocities in these simulations; hence, the Δv^{max} criterion provides upper and lower limits on the line-of-sight distance to companions. Also, recall from the preceding section that the choice of M_1 has no effect on the pair statistics if clustering is independent of luminosity. Hence, we choose $M_1=M_2$, which maximizes the size of the primary sample, and therefore minimizes the measurement errors in N_c and L_c .

With these assumptions, we compute pair statistics for a range of choices of M_2 . Errors are computed using the Jackknife technique. For this resampling method, partial standard deviations, δ_i , are computed for each object by taking the difference between the quantity being measuring, f , and the same quantity with the i^{th} galaxy removed from the sample, f_i , such that $\delta_i = f - f_i$. For a sample of N galaxies, the variance is given by $[(N-1)/N \sum_i \delta_i^2]^{1/2}$ (Efron 1981; Efron & Tibshirani 1986). Results are given in Figure 1. Both statistics continue to increase as M_2 becomes fainter. N_c diverges at faint magnitudes, while L_c is seen to converge. This behaviour is a direct consequence of the shape of the LF; N_c converges for $\alpha > -1$, while L_c converges for $\alpha > -2$. The existence and magnitude of these trends clearly demonstrate the need to specify M_2 when measuring pair statistics.

6. APPLICATION TO FLUX-LIMITED SAMPLES

The preceding section gives a straightforward prescription for computing pair statistics in volume-limited samples. However, redshift surveys are generally flux-limited. By defining a volume-limited sample within such a survey, one must discard a large proportion of the data. In this section, we will outline how these pair statistics can be applied to flux-limited surveys.

Pair statistics necessarily depend on both clustering and mean density, as shown by Equations 15 and 16. In a flux-limited sample, both clustering and mean density will vary throughout the sample. We will use these equations to account for redshift-dependent changes in mean density, and we will demonstrate how to minimize the effects of clustering differences. These techniques will then be tested with Monte Carlo simulations.

6.1. Dependence on Clustering

By removing the fixed luminosity limit, the overall distribution of galaxy luminosities will vary with redshift within the sample, and the mean luminosity of the sample will differ from the volume-limited sample. However, galaxy clustering is known to be luminosity dependent. Measures of the galaxy correlation function (e.g., Loveday et al. 1995, Willmer et al. 1998), power spectrum (e.g., Vogeley 1993), and counts in cells (Benoist et al. 1996) all find that luminous galaxies ($L > L_*$) are more clustered

than sub- L_* galaxies, typically by a factor of ~ 2 . This increase in clustering may be particularly strong (factor ~ 4) for very luminous galaxies ($M_B < -21$).

Clearly, this effect should not be ignored when computing pair statistics. In principle, this could be incorporated into the measurement of these pair statistics. However, available pair samples are too small to measure this dependence. We choose instead to minimize these effects by restricting the analysis to a fixed range in absolute magnitude, within which luminosity-dependent clustering is small or negligible. This is done by imposing additional bright (M_{bright}) and faint (M_{faint}) absolute magnitude limits on the sample. Having thereby reduced the effects of luminosity segregation, we then assume that the remaining differences will not have a significant effect on the measured pair statistics. In Section 8.3, we use the SSRS2 sample to demonstrate empirically that this is in fact a reasonable assumption.

6.2. Dependence on Limiting Absolute Magnitude

In Section 5, we demonstrated that these pair statistics are meaningful only if one specifies the minimum luminosity of the primary and secondary samples. For a flux-limited sample, however, the minimum luminosity of the sample increases with redshift. One must therefore decide on a representative minimum luminosity, and account for differences between the desired minimum luminosity and the redshift-dependent minimum imposed by the apparent magnitude limit of the sample. If the LF is known, this can be achieved by weighting each galaxy appropriately. In this section, we outline a weighting scheme which makes this correction.

6.2.1. Weighting of Secondary Sample

Consider a flux-limited sample in which host galaxies are located at a variety of redshifts. Those at low redshift will have the greatest probability of having close companions that lie above the flux limit, since the flux limit corresponds to an intrinsic luminosity that is fainter than that for galaxies at higher redshift. If we wish to avoid an inherent bias in the pair statistics, we must correct for this effect. Furthermore, we must account for any limits in absolute magnitude imposed on the sample to reduce the effects of luminosity-dependent clustering (§ 6.1). Finally, we have demonstrated the importance of specifying a limiting absolute magnitude for companions (M_2) when computing pair statistics. Therefore, we must attempt to correct the pair statistics to the values that would have been achieved for a volume-limited secondary sample with $M_{\text{bright}} \leq M \leq M_2$. Qualitatively, this correction should assign greater importance (or weight) to the more rare companions found at the high redshift end of the flux-limited sample. To make this correction as rigorous as possible, we will use the galaxy LF. By integrating the LF over a given range in absolute magnitude, one can obtain an estimate of the mean number or luminosity density of galaxies in the sample. By performing this integration at any given redshift, accounting for the allowed ranges in absolute magnitude and the flux limit, it is possible to quantify how the mean density varies with redshift within the defined sample. This information can be used to remove this unwanted bias from the pair statistics.

We assign a weight to each galaxy in the secondary sample, which renormalizes the sample to the density corresponding to $M_{\text{bright}} \leq M \leq M_2$. We must first determine $M_{\text{lim}}(z_i)$, which gives the limiting absolute magnitude allowed at redshift z_i . At most redshifts, this is imposed by the limiting apparent magnitude m , such that $M_{\text{lim}}(z_i) = m - 5 \log d_L(z) - 25 - k(z)$. At the low redshift end of the sample, however, M_{faint} (defined in § 6.1) will take over. That is, the limiting absolute magnitude used for identifying galaxies in the secondary sample is given by

$$M_{\text{lim}}(z_i) = \max[M_{\text{faint}}, m - 5 \log d_L(z) - 25 - k(z)]. \quad (19)$$

The selection function, denoted $S(z)$, is defined as the ratio of densities in flux-limited versus volume-limited samples. This function, given in terms of number density ($S_N(z)$) and luminosity density ($S_L(z)$), is as follows :

$$S_N(z_i) = \frac{\int_{M_{\text{bright}}}^{M_{\text{lim}}(z_i)} \phi(M) dM}{\int_{M_{\text{bright}}}^{M_2} \phi(M) dM} \quad (20)$$

$$S_L(z_i) = \frac{\int_{M_{\text{bright}}}^{M_{\text{lim}}(z_i)} \phi(M) L(M) dM}{\int_{M_{\text{bright}}}^{M_2} \phi(M) L(M) dM}, \quad (21)$$

where $L(M)$ is defined in Equation 13. In order to recover the correct pair statistics, each companion must be assigned weights $w_{N2}(z_i) = 1/S_N(z_i)$ and $w_{L2}(z_i) = 1/S_L(z_i)$. The total number and luminosity of close companions for the i^{th} primary galaxy, computed by summing over the j galaxies satisfying the ‘‘close companion’’ criteria, is given by $N_{c_i} = \sum_j w_{N2}(z_j)$ and $L_{c_i} = \sum_j w_{L2}(z_j) L_j$ respectively. By applying this weighting scheme to all galaxies in the secondary sample, we will retrieve pair statistics that correspond to a volume-limited sample with $M_{\text{bright}} \leq M \leq M_2$.

6.2.2. Weighting of Primary Sample

The above weighting scheme ensures that the number and luminosity of companions found around each primary galaxy is normalized to $M_{\text{bright}} \leq M \leq M_2$. However, these estimates are obviously better for galaxies at the low redshift end of the primary sample, since they will have the largest number of *observed* companions. Recall that N_c and L_c are quantities that are averaged over a sample of primary galaxies. In order to minimize the errors in these statistics, we assign weights to the primary galaxies (denoted $w_{N1}(z_i)$ and $w_{L1}(z_i)$) which are inversely proportional to the square of their uncertainty. If the observed number and luminosity of companions around the i^{th} primary galaxy are given by $N_i(\text{obs})$ and $L_i(\text{obs})$ respectively, and if we assume that the uncertainties are determined by Poisson counting statistics, then $N_{c_i} = w_{N2}(z_i) N_i(\text{obs}) \pm w_{N2}(z_i) \sqrt{N_i(\text{obs})}$ and $L_{c_i} = w_{L2}(z_i) L_i(\text{obs}) \pm w_{L2}(z_i) \sqrt{L_i(\text{obs})}$. On average, these quantities will be related to expectation values $\langle N_c \rangle$ and $\langle L_c \rangle$ by $\langle N_c \rangle = w_{N2}(z_i) N_i(\text{obs})$ and $\langle L_c \rangle = w_{L2}(z_i) L_i(\text{obs})$. Combining these relations yields

$$w_{N1}(z_i) = \frac{1}{N_i(\text{obs}) w_{N2}(z_i)^2} = \frac{1}{\langle N_c \rangle w_{N2}(z_i)} \propto w_{N2}(z_i)^{-1} \quad (22)$$

$$w_{L1}(z_i) = \frac{1}{L_i(obs)w_{L2}(z_i)^2} = \frac{1}{\langle L_c \rangle w_{L2}(z_i)} \propto w_{L2}(z_i)^{-1} \quad (23)$$

That is, the optimal weighting is the reciprocal of the weighting scheme used for companions. Therefore, weights $w_{N1}(z_i) = S_N(z_i)$ and $w_{L1}(z_i) = S_L(z_i)$ should be assigned to primary galaxies. The pair statistics are then computed as follows :

$$N_c = \frac{\sum_i w_{N1}(z_i) N_{c_i}}{\sum_i w_{N1}(z_i)} \quad (24)$$

$$L_c = \frac{\sum_i w_{L1}(z_i) L_{c_i}}{\sum_i w_{L1}(z_i)}. \quad (25)$$

It is worth noting that, for a close pair, both galaxies will lie at roughly the same redshift, meaning that $w_1(z_i) \times w_2(z_j) \approx 1$. We choose not to make this approximation, in order to keep these relations valid for pairs that are not close, and to allow for future application to pairs with additional selection weights. However, we stress that, with or without this approximation, the primary weights in the denominator provide an overall correction for the flux limit, unlike the traditional pair fraction. Note also that, for a volume-limited sample, weights for all galaxies in the primary and secondary samples are equal, reducing these equations to $N_c = \sum N_{c_i}/N_1$ and $L_c = \sum L_{c_i}/N_1$, as defined in Section 5.1.

6.2.3. Boundary Effects

A small correction must be made to these weights if a primary galaxy lies close to a region of space that is not covered by the survey. This will happen if a galaxy lies close to the boundaries on the sky, or close to the minimum or maximum redshift allowed. If this is the case, it is possible that close companions will be missed, leading to an underestimate of the pair statistics. Therefore, we must account for these effects.

First, we consider galaxies lying close to the survey boundaries on the sky, as defined in Section 3. For each galaxy in the primary sample, we compute the fraction of sky with $r_p^{\min} \leq r_p \leq r_p^{\max}$ that lies within the survey boundaries. This fraction will be denoted f_b . For SSRS2, our usual choices of r_p^{\min} and r_p^{\max} (see § 7) make this a very small effect, with $f_b=1$ for 99.75% of galaxies in the primary sample. Having measured f_b for each galaxy in the primary sample, we must incorporate this into the measurement of the pair statistics. The first task is to ensure that we correct the number of companions to match what would be expected if coverage was complete. We do this by assigning each companion a boundary weight $w_{b2} = 1/f_b$, where f_b is associated with its host galaxy from the primary sample. By multiplying each companion by its boundary weight, we will recover the correct number of companions. We must also adjust weights for the primary galaxies. Following the method described in the previous section, we wish to give less weight to galaxies that are likely to have fewer observed companions. Therefore, each primary galaxy is assigned a boundary weight $w_{b1} = f_b$.

We now consider galaxies which lie near the survey boundaries along the line of sight. If a primary galaxy

lies close to the minimum or maximum redshift allowed, it is possible that we will miss companions because they lie just across this redshift boundary. In order to account correctly for this effect, one would need to model the velocity distribution of companions. As this requires several assumptions, we choose instead to exclude all companions that lie between a primary galaxy and its nearest redshift boundary, provided the boundary lies within Δv^{\max} of the primary galaxy. To account for this exclusion, we assume that the velocity distribution is symmetric along the line of sight. Thus, as we will miss half of the companions for these galaxies, we assign a weight of $w_{v2}=2$ to any companions found in the direction opposite to the boundary. We must also consider how to weight the primary galaxies themselves. Clearly, primary galaxies close to the redshift boundaries will be expected to have half as many *observed* companions as other primary galaxies. To minimize the errors in computing the pair statistics, we assign these primary galaxies weights $w_{v1}=0.5$.

To summarize, weights for companions in the secondary sample are given by

$$w_{N2} = S_N(z_i)^{-1} w_{b2} w_{v2}, \quad (26)$$

$$w_{L2} = S_L(z_i)^{-1} w_{b2} w_{v2}, \quad (27)$$

while primary galaxies are assigned weights

$$w_{N1} = S_N(z_i) w_{b1} w_{v1}, \quad (28)$$

$$w_{L1} = S_L(z_i) w_{b1} w_{v1}. \quad (29)$$

6.3. Confirmation Using Monte Carlo Simulations

We will now perform a test to see if this weighting scheme achieves the desired effects. To do this, we will use flux-limited Monte Carlo simulations, for which the intrinsic density and clustering are fixed. Therefore, the *intrinsic* pair statistics do not depend on redshift or luminosity. If the secondary sample weights are correct, the measured pair statistics will be the same everywhere (within the measurement errors), regardless of redshift or luminosity. We will also check to see if the weights for the primary sample are correct. If they are, the errors on the pair statistics will be minimized, as desired.

The flux-limited Monte Carlo simulations were generated in a similar manner to the simulations described in Section 5.4; however, a limiting apparent magnitude of $m_B \leq 15.5$ was imposed. Sample sizes of 8000 (South) and 4035 (North) were used, providing a good match to the overall density in SSRS2. The resulting simulations are similar to SSRS2 in all respects, except for the absence of clustering. We have already established how the pair statistics depend on the choice of M_1 and M_2 . In the following analysis, we choose $M_2=M_1=-19$. In Section 6.1, we outlined reasons for restricting the sample to a fixed range in absolute magnitude. Here, we demonstrate how the chosen range affects N_c and L_c . For comparison, we also compute N_c without normalizing to a specified range in absolute magnitude (in this case, $w_{N1}=w_{L1}=1$). This provides some insight into the behaviour of the traditional (uncorrected) pair fraction.

These tests are most straightforward if the intrinsic pair statistics are the same everywhere in the enclosed volume. This is not quite true for these simulations, however. Galaxies are distributed randomly within the enclosed *comoving* volume. As a result, the physical density varies with redshift as $(1+z)^3$. In addition, the volume element encompassed by the line-of-sight pair criterion Δv varies with redshift as $(1+z)^{-3/2}$ for $q_0=0.5$. In order to have the simulations mimic a sample with universal pair statistics, we normalize the sample for these effects by weighting each galaxy by $(1+z)^{-3/2}$. We stress that this is done only for the Monte Carlo simulations. One should *not* apply either of these corrections to real redshift data.

In Figure 2, the pair statistics are computed for a range of M_{faint} . In addition, we compute N_c without weighting by the luminosity function, to demonstrate the danger of ignoring this important correction. This statistic is directly analogous to the traditional (uncorrected) pair fraction used in the literature. It is clear that both N_c and L_c are independent of the choice of M_{faint} , within the errors. This verifies that we have correctly accounted for the biases introduced by the apparent magnitude limit. In contrast, the unweighted N_c is seen to have a strong dependence on M_{faint} . As expected, it increases as M_{faint} becomes fainter, due to the increase in sample density. We stress that this does not happen with the normalized N_c and L_c statistics, because both are corrected to a fixed range in limiting absolute magnitude.

Finally, we demonstrate that the weighting scheme used for the primary sample (§ 6.2.2) does in fact minimize errors in N_c and L_c . Recall that the weighting used was the reciprocal of the weights for the secondary sample. Here we will assume that $w_{N1} \propto w_{N2}(z_i)^x$ and $w_{L1} \propto w_{L2}(z_i)^x$. In Section 6.2.2, justification was given for setting $x=-1$. Here, we will allow x to vary, in order to investigate empirically which value minimizes the errors. Special cases of interest are $x=0$ (no weighting) and $x=1$ (same weighting as *secondary* sample). The results are given in Figure 3. The relative errors in N_c and L_c reach a minimum at $x \sim -1$, as expected. Errors are $\sim 40\%$ larger if no weighting is used ($x=0$). For $x=1$, errors are much larger, increasing by nearly a factor of 5. While errors increase dramatically for $x \geq 0$, they change slowly around $x=-1$. Clearly, $x=-1$ is an excellent choice.

7. A PAIR CLASSIFICATION EXPERIMENT

The first step in applying these techniques to a real survey of galaxies is to decide on a useful close pair definition. This involves imposing a maximum projected physical separation (r_p^{max}) and, if possible, a maximum line-of-sight rest-frame velocity difference (Δv^{max}). The limits should be chosen so as to extract information on mergers in an optimal manner. This involves a compromise between the number and merging likelihood of pairs. While one should focus on companions which are most likely to be involved in mergers, a very stringent pair definition may yield a small and statistically insignificant sample.

In previous close pair studies, the convention has been to set $r_p^{\text{max}} = 20 h^{-1}$ kpc. Pairs with separations of $r_p \leq 20 h^{-1}$ kpc are expected to merge within 0.5 Gyr (e.g., Barnes 1988, Patton et al. 1997). We note, however, that timescale estimates are approximate in nature, and have

yet to be verified. In earlier work, it has not been possible to apply a velocity criterion, since redshift samples have been too small to yield useful pair statistics using only galaxies with measured redshifts. Instead, all physical companions have been used, with statistical correction for optical contamination (Patton et al. 1997). With a complete redshift sample, we can improve on this. This can be seen by inspecting a plot of r_p versus Δv for the SSRS2 pairs, given in Figure 4. By imposing a velocity criterion, we can eliminate optical contamination; furthermore, we are able to concentrate on the physical pairs with the lowest relative velocities, and hence the greatest likelihood of merging.

We can now use our large sample of low- z pairs to shed new light on these issues. We will use images of these pairs in an attempt to determine how signs of interactions are related to pair separation. We begin by finding all 255 SSRS2 pairs with $r_p \leq 100 h^{-1}$ kpc, computing r_p and Δv for each. Images for these pairs were extracted from the Digitized Sky Survey. Interactions were immediately apparent in some of these pairs, and the images were deemed to be of sufficient quality that a visual classification scheme would be useful. An interaction classification parameter (I_c) was devised, where $I_c=0$ indicates that a given pair is “definitely not interacting”, and $I_c=10$ indicates “definitely interacting”. In order to avoid a built-in bias, the classifier is not given the computed values of r_p and Δv . The classifier uses all visible information available (tidal tails and bridges, distortions/asymmetries in member galaxies, apparent proximity, etc.). Classifications were performed by three of us (DRP, ROM, RGC), and the median classification was determined for each system. The results are presented in Figure 5. A clickable version of this plot, which allows the user to see the corresponding Digitized Sky Survey image for each pair, is available at <http://www.astro.utoronto.ca/~patton/ssrs2/Ic>.

There are several important features in this plot. First, there is a clear correlation between I_c and r_p , with closer pairs exhibiting stronger signs of interactions. There are several interacting pairs with $r_p \sim 50 h^{-1}$ kpc. While these separations are fairly large, it is not surprising that there would be some early-stage mergers with these separations (e.g., Barton, Bromley, & Geller 1998). An excellent example of this phenomenon is the striking tail-bridge system Arp 295a/b (cf. Hibbard & van Gorkom 1996), which has $r_p = 95 h^{-1}$ kpc. However, these systems clearly do not dominate; almost all pairs with large separations have very low interaction classifications. The majority of pairs showing clear signs of interactions/mergers have $r_p \lesssim 20 h^{-1}$ kpc.

There is also a clear connection with Δv . Pairs with $\Delta v > 600$ km/s do not exhibit signs of interactions, with 61/63 (97%) classified as $I_c \leq 1$. This indicates that interactions are most likely to be seen in low velocity pairs, as expected. We note, however, that there are very few optical pairs (i.e., small r_p and large Δv) in this low redshift sample. At higher redshift, increased optical contamination may lead to difficulties in identifying interacting systems when the galaxies are close enough to have overlapping isophotes. Clearly, it is necessary to have redshift information for both members of each pair if one is to exclude these close optical pairs.

After close inspection of Figure 5, we decided on close pair criteria of $r_p^{\max} = 20 h^{-1} \text{ kpc}$ and $\Delta v^{\max} = 500 \text{ km/s}$. A mosaic of some of these pairs is given in Figure 6. In this regime, 31% (9/29) exhibit convincing evidence for interactions ($I_c \geq 9$), while 69% (20/29) show some indication of interactions ($I_c \geq 6$). Furthermore, the vast majority (9/10) of pairs with clear signs of interactions ($I_c \geq 9$) are found in this regime. These criteria appear to identify a sample of pairs which are likely to be undergoing mergers; moreover, the resulting sample includes most of the systems classified as interacting.

We also impose an inner boundary of $r_p = 5 h^{-1} \text{ kpc}$. This limit is chosen so as to avoid the confusion that is often present on the smallest scales. In this regime, it is often difficult to distinguish between small galaxies and sub-galactic units, particularly in merging systems. While we are omitting the most likely merger candidates, those at separations $< 5 h^{-1} \text{ kpc}$ are not expected to account for more than $\sim 5\%$ of the companions within $20 h^{-1} \text{ kpc}$. This expectation, which has yet to be verified, is based both on pair counts in *HST* imaging (Burkey et al. 1994) and on inward extrapolation of the correlation function (Patton et al. 1997). While this inner boundary will lead to a slight decrease in N_c and L_c , it should have no significant effect on estimates of merger/accretion rate evolution, provided the same restriction is applied to comparison samples at other redshifts.

8. APPLICATION TO SSRS2

In the preceding sections, we have outlined techniques for measuring pair statistics in a wide variety of samples. We have demonstrated a robust method of applying this approach to flux-limited samples, accounting for redshift-dependent density changes and minimizing differences in clustering. We have also selected pair definitions that identify the most probable imminent mergers. We will now apply these techniques to the SSRS2 survey. As this is a complete redshift survey, redshifts are available for all close companions; hence, for the first time, we will measure pair statistics using only close *dynamical* pairs. After limiting the analysis to a reasonable range in absolute magnitude, we compute N_c and L_c for the SSRS2 survey.

8.1. Defining Survey Parameters

In Section 6.1, we emphasized the importance of restricting the sample in absolute magnitude, to minimize bias due to luminosity-dependent clustering. For SSRS2, we first impose a bright limit of $M_{\text{bright}} = -21$. All galaxies brighter than this are hereafter excluded from the analysis. This allows us to avoid the most luminous galaxies, which are probably the most susceptible to luminosity-dependent clustering; however, this reduces the size of the sample by only 0.5%. We also impose a faint absolute magnitude limit of $M_{\text{faint}} = -17$, which results in the exclusion of intrinsically faint galaxies at $z \lesssim 0.01$. This guards against the possibility that these intrinsically faint galaxies are clustered differently than the bulk of the galaxies in the sample. This pruning of the sample is illustrated in Figure 7. These restrictions allow us to minimize concerns about luminosity-dependent clustering while retaining 90% of the sample. The final results are insensitive to these particular choices (see Section 8.3).

The above limits in absolute magnitude, along with the flux limit, define the usable sample of galaxies. In order to compute pair statistics, we must also normalize the measurements to a given range in absolute magnitude, for both the primary and secondary samples. The mean limiting absolute magnitude of the primary sample, weighted according to Section 6.2.2, is $M_B = -17.8$. For convenience, we set $M_2(B) = -18.0$ (we will compute pair statistics for $-19 \leq M_2(B) \leq -17$ in the following section). For reference, we note that this corresponds to $m_B = 15.5$ at $z = 0.017$. As we are dealing with a complete redshift sample, we set $M_1(B) = M_2(B)$ in order to use all of the available information. Finally, as we have limited the sample using $M_{\text{bright}} = -21$, this will be used in conjunction with $M_2(B)$ to derive pair statistics for galaxies with $-21 \leq M_B \leq -18$.

8.2. SSRS2 Pair Statistics

Using these parameters, we identified all close companions in SSRS2. The North sample yielded 27 companions, and 53 were found in the South, giving a total of 80. We emphasize that it is *companions* that are counted, rather than pairs; hence, if both members of a pair fall within the primary sample, the pair will usually yield 2 companions. A histogram of companion absolute magnitudes is given in Figure 8. This plot shows that 90% of the companions we observe in our flux-limited sample fall in the range $-21 \leq M_B \leq -18$. Hence, galaxies with $-18 \leq M_B \leq -17$ do not dominate the sample. Tables 2 and 3 give complete lists of close aggregates (pairs and triples) for SSRS2 North and South respectively. These systems contain all companions used in the computation of pair statistics. These tables list system ID, number of members, r_p ($h^{-1} \text{ kpc}$), Δv (km/s), RA (1950.0), DEC (1950.0), and recession velocity (km/s). DSS images for these systems were given earlier in Figure 6.

Using this sample of companions, the pair statistics were computed. The results are given in Table 1. Errors were computed using the Jackknife technique. Results from the two subsamples were combined, weighting by Jackknife errors, to give $N_c = 0.0226 \pm 0.0052$ and $L_c = 0.0216 \pm 0.0055 \times 10^{10} h^2 L_\odot$ at $z = 0.015$. Results from the two subsamples agree within the quoted 1σ errors.

To facilitate future comparison with other samples, we also generate pair statistics spanning the range $-19 \leq M_2(B) \leq -17$ (see Table 4). We note, however, that while we account for changes in number and luminosity density over this luminosity range (using LF weights described in Section 6), there is no correction for changes in clustering. Hence, our statistics should be considered most appropriate for $M_2(B) = -18$, and more approximate in nature at brighter and fainter levels. The results in Table 4 indicate that N_c increases by a factor of 5 between $M_2(B) = -19$ and $M_2(B) = -17$, resulting solely from an increase in mean number density. The change in L_c is less pronounced, with an increase by a factor of 2 over the same luminosity range. These substantial changes in both statistics emphasize the need to specify M_2 when computing pair statistics and comparing results from different samples. In addition, the smaller change in L_c is indicative of the benefits of using a luminosity statistic such as

L_c , which is more likely to converge as one goes to fainter luminosities (see Section 5.4). L_c will always converge faster than N_c , thereby reducing the sensitivity to M_2 . Furthermore, it is possible to retrieve most of the relevant luminosity information without probing to extremely faint levels. For example, for the SSRS2 LF, 70% of the total integrated luminosity density is sampled by probing down to $M_2(B) = -18$. To first order, the same will be true for L_c . Going 2 magnitudes fainter would increase the completeness to 95%. While we are currently unable to apply pair statistics down to these faint limits, this will be pursued when deeper surveys become available.

8.3. Sensitivity of Results to Survey Parameters

In this section, we explore the effects of choosing different survey parameters. Earlier in this study, we demonstrated that N_c and L_c are insensitive to the choice of survey limits in absolute magnitude, provided clustering is independent of luminosity and the pair statistics are normalized correctly. Here, we test this hypothesis empirically.

First, we compute the pair statistics for a range in M_{faint} , normalizing the statistics to $-21 \leq M_B \leq -18$ in each case. Figure 9 demonstrates a possible trend of decreasing pair statistics with fainter M_{faint} . This trend, however, is significant only for the brightest galaxies ($M_{\text{faint}} \lesssim -19$). This is consistent with the findings of Willmer et al. (1998), who measure an increase in clustering for bright galaxies in SSRS2, on scales of $r_p > 1 h^{-1}$ Mpc. For fainter M_{faint} , there is no significant dependence. The pair statistics vary by $\sim 5\%$ over the range $-17.5 \leq M_{\text{faint}} \leq -16.5$, which is well within the error bars. Therefore, we conclude that our choice of $M_{\text{faint}} = -17$ has a negligible effect on N_c and L_c . This implies that, to first order, clustering is independent of luminosity within this sample.

Next, we investigate how the pair statistics depend on our particular choices of r_p^{max} and Δv^{max} , which comprise our definition of a close companion. First, we compute pair statistics for $10 h^{-1} \text{ kpc} \leq r_p^{\text{max}} \leq 100 h^{-1} \text{ kpc}$, with $\Delta v^{\text{max}} = 500 \text{ km/s}$. Results are given in Figure 10. This plot indicates a smooth increase in both statistics with r_p^{max} . This trend is expected from measurements of the galaxy CF. The CF is commonly expressed as a power law of the form $\xi(r, z) = (r_0/r)^\gamma$, with $\gamma=1.8$ (Davis & Peebles 1983). Integration over this function yields pair statistics that vary as $r_p^{3-\gamma} \approx r_p^{1.2}$, which is in good agreement with the trend found in Figure 10. From this plot, it also appears likely that there are systematic differences between the two subsamples. This is hardly surprising, since there are known differences in density between the subsamples, and it is likely that there are non-negligible differences in clustering as well. This cosmic variance is not currently measurable on the smaller scales ($r_p \leq 20 h^{-1} \text{ kpc}$) relevant to our main pair statistics. Hence, we choose to ignore these differences for now. However, these field-to-field variations are certain to add some systematic error to our quoted pair statistics.

We also compute pair statistics for a range in Δv^{max} . This is done first for $r_p^{\text{max}} = 20 h^{-1} \text{ kpc}$, showing the relative contributions at different velocities to the main pair statistics quoted in this paper. We also compute statis-

tics using $r_p^{\text{max}} = 100 h^{-1} \text{ kpc}$, in order to improve the statistics. Results are given in Figure 11. Several important conclusions may be drawn from this plot. First, at small velocities ($\Delta v^{\text{max}} \lesssim 700 \text{ km/s}$), both pair statistics increase with Δv^{max} , as expected. This simply indicates that one continues to find additional companions as the velocity threshold increases. Secondly, it appears that our choice of Δv^{max} was a good one. The $r_p \leq 20 h^{-1} \text{ kpc}$ pair statistics increase very little beyond $\Delta v^{\text{max}} = 500 \text{ km/s}$, while the contamination due to non-merging pairs would continue to increase (see Figure 4). Moreover, as both pair statistics flatten out at around $\Delta v^{\text{max}} = 500 \text{ km/s}$, small differences in the velocity distributions of different samples should not result in large differences in their pair statistics. Finally, for $r_p^{\text{max}} \leq 100 h^{-1} \text{ kpc}$, the pair statistics continue to increase out to $\sim 2000 \text{ km/s}$. This indicates an increase in velocity dispersion at these larger separations. This provides additional confirmation that one is less likely to find low-velocity pairs at larger separations, thereby implying that mergers should also be less probable.

9. DISCUSSION

9.1. Comparison with Earlier Estimates of the Local Pair Fraction

All published estimates of the local pair fraction have been hindered by small sample sizes and a lack of redshifts. In addition, as demonstrated throughout this paper, the traditional pair fraction is not a robust statistic, particularly when applied to flux-limited surveys. The new statistics introduced in this paper, along with careful accounting for selection effects such as the flux limit, yield the first secure measures of pair statistics at low redshift. Therefore, strictly speaking, the results in this paper cannot be compared directly with earlier pair statistics. However, it is possible to check for general consistency in results, and we will attempt to do so.

As discussed in Section 2, Patton et al. (1997) estimated the local pair fraction to be $4.3 \pm 0.4\%$, using the UGC catalog. The Patton et al. (1997) estimate was based on a flux-limited sample with $B \leq 14.5$, and a mean redshift of $z=0.0076$. This corresponds roughly to an average limiting absolute magnitude of $M_B = -17.3$. Loosely speaking, this is analogous to M_2 . The pair definition used in their estimate was $r_p \leq 20 h^{-1} \text{ kpc}$, with no Δv criterion. N_c may be interpreted as an approximation to the traditional pair fraction, provided the relative proportion of triples is small. We recompute the SSRS2 pair statistics, using $\Delta v^{\text{max}} = 1000 \text{ km/s}$ in an attempt to match the results that would be found using no Δv criterion (see Figure 11). We find $N_c = 0.026 \pm 0.006$. This implies a local pair fraction of $2.6 \pm 0.6\%$. This value is somewhat smaller than the earlier result, with larger errors. We strongly emphasize that, while these results are broadly consistent, we would not expect excellent agreement, due to the improved techniques used in this study.

9.2. The Merger Fraction at $z \sim 0$

The quantities N_c and L_c are practical measures of the average numbers and luminosities of companions with relatively high merging probabilities. However, the ambi-

guity of redshift space is such that some of these companions can be entirely safe from ever merging. That is, $\Delta v = 500$ km/s can correspond either to two galaxies at a small physical separation with a large infall velocity, or, to two galaxies at a separation of $5h^{-1}$ Mpc, with no relative peculiar velocity. In order to transform from N_C (and L_C) to an estimate of the incidence of mergers, we must determine what fraction of our close companions have true 3-dimensional physical separations of $r < 20 h^{-1}$ kpc. This quantity, which we refer to as f_{3D} , has been discussed previously by Yee and Ellingson (1995). This quantity needs to be evaluated based on the small separation clustering and kinematics of the galaxy population, r_0 , γ , and σ_{12} , the parameters Δv and r_p^{\max} , and the projected separation at which two galaxies “optically overlap” in the image. The quantity f_{3D} is then evaluated with a triple integral, first placing the correlation function into redshift space, then integrating over projected and velocity separation. For reasonable choices of pair selection parameters, the outcome is fairly stable at $f_{3D} \simeq 0.5$. The most important parameter is $\Delta V/\sigma_{12}$, which should lie in the range of 2 to 4. If this parameter is too small, physical pairs will be missed; if it is too large, too many distant companions will be incorporated. Other reasonable choices include setting the ratio of the overlap separation to maximum pair separation to be at least three, and the ratio of the maximum pair separation to correlation length to be at least a factor of 30. We will take $f_{3D}=0.5$ to be the best estimate currently available.

We can now estimate the merger fraction (f_{mg}) at the present epoch. In this study, we have found $N_C=0.0226\pm 0.0052$. As most companions are found in pairs, rather than triplets or higher order N-tuples, this is comparable to the fraction of galaxies in close pairs. From our estimate of f_{3D} , we infer that half of these galaxies are in merging systems, yielding $f_{\text{mg}} \approx 0.011$. This implies that approximately 1.1% of $-21 \leq M_B \leq -18$ galaxies are undergoing mergers at the present epoch. We stress here that this result applies only to galaxies within the specified absolute magnitude limits. Probing to fainter luminosities would cause f_{mg} to increase substantially. In addition, this result applies only to the close companions defined in this analysis. Clearly, by modifying this definition (and therefore changing the typical merger timescale under consideration), the merger fraction would also be certain to change.

9.3. The Merger Timescale

We now have an idea of how prevalent ongoing mergers are at the present epoch. In order to relate this result to the overall importance of mergers, we must estimate the merger timescale (T_{mg}). We will use the properties of our SSRS2 pairs to estimate the mean dynamical friction timescale for pairs in our sample. Following Binney and Tremaine (1987), we assume circular orbits and a dark matter density profile given by $\rho(r) \propto r^{-2}$. The dynamical friction timescale T_{fric} (in Gyr) is given by

$$T_{\text{fric}} = \frac{2.64 \times 10^5 r^2 v_c}{M \ln \Lambda}, \quad (30)$$

where r is the initial physical pair separation in kpc, v_c is the circular velocity in km/s, M is the mass (M_\odot), and

$\ln \Lambda$ is the Coulomb logarithm. We estimate r and v_c using the pairs in Tables 2 and 3. The mean projected separation is $r_p \sim 14h^{-1}$ kpc. As our procedure already includes a correction from projected separation (r_p) to 3-dimensional separation (r), we take $r = r_p$. Assuming $h=0.7$, this leads to $\bar{r} \sim 20$ kpc. The mean line of sight velocity difference is $\Delta v \sim 150$ km/s. We assume the velocity distribution is isotropic, which implies that $v_c = \sqrt{3}\Delta v \sim 260$ km/s. The mean absolute magnitude of companions is $M_B \sim -19$ (see Figure 8). We assume a representative estimate of the galaxy mass-to-light ratio of $M/L \sim 5$, yielding a mean mass of $M \sim 3 \times 10^{10} M_\odot$. Finally, Dubinski, Mihos, and Hernquist (1999) estimate $\ln \Lambda \sim 2$, which fits the orbital decay of equal mass mergers seen in simulations. Using Equation 30, we find $T_{\text{fric}} \sim 0.5$ Gyr. We caution that this estimate is an approximation, and is averaged over systems with a wide range in merger timescales. Nevertheless, we will take $T_{\text{mg}} = 0.5$ Gyr as being representative of the merger timescale for the pairs in our sample.

9.4. The Cumulative Effect of Mergers Since $z \sim 1$

Now that we have estimated the present epoch merger fraction and the merger timescale, we will attempt to ascertain what fraction of present galaxies have undergone mergers in the past. These galaxies can be classified as merger remnants; hence, we will refer to this fraction as the remnant fraction (f_{rem}). We begin by imagining the state of affairs at a lookback time of $t = T_{\text{mg}}$. Suppose the merger fraction at the corresponding redshift is given by $f_{\text{mg}}(z)$. In the time interval between then and the present, a fraction $f_{\text{mg}}(z)$ of galaxies will undergo mergers, yielding $0.5f_{\text{mg}}(z)$ merger remnants. Therefore, the remnant fraction at the present epoch is given by

$$f_{\text{rem}} = 1 - \frac{1 - f_{\text{mg}}(z)}{1 - 0.5f_{\text{mg}}(z)}. \quad (31)$$

Similarly, if we extend this to a lookback time of NT_{mg} , where N is an integer, then the remnant fraction is given by

$$f_{\text{rem}} = 1 - \prod_{j=1}^N \frac{1 - f_{\text{mg}}(z_j)}{1 - 0.5f_{\text{mg}}(z_j)}, \quad (32)$$

where z_j corresponds to a lookback time of $t = jT_{\text{mg}}$. We now make the simple assumption that the merger rate does not change with time. In this case, our present epoch estimate of the merger fraction holds at all redshifts, giving $f_{\text{mg}}(z)=0.011$. In order to convert between redshift and lookback time, we must specify a cosmological model. We assume a Hubble constant of $h=0.7$. For simplicity, we assume $q_0=0.5$. Therefore, $z = (1 - 3H_0 t/2)^{-2/3} - 1$. Using our merger timescale estimate of $T_{\text{mg}}=0.5$ Gyr, we can now investigate the cumulative effect of mergers. With the chosen cosmology, $z=1$ corresponds to a lookback time of ~ 6 Gyr, or $12T_{\text{mg}}$ ($N=12$). With this lookback time, Equation 32 yields $f_{\text{rem}}=0.066$. This implies that $\sim 6.6\%$ of galaxies with $-21 \leq M_B \leq -18$ have undergone mergers since $z \sim 1$.

If the mergers taking place in our sample produce elliptical galaxies, it is worthwhile comparing the remnant fraction to the elliptical fraction (cf. Toomre 1977). The

elliptical fraction for bright field galaxies is generally found to be about 10% (e.g., Dressler 1980, Postman and Geller 1984). This result is broadly consistent with the remnant fraction found in this study.

While our estimate of the remnant fraction is based on our statistically secure measurement of N_C , it also relies on fairly crude assumptions regarding the merger fraction and merger timescale. In particular, the merger rate has been assumed to be constant. There is no physical basis for this assumption; in fact, a number of studies have predicted a rise in the merger rate with redshift. If this is true, we will have underestimated the remnant fraction, and the relative importance of mergers. In a future paper (Patton et al. 2000), we will address this issue by investigating how the merger rate changes with redshift.

10. CONCLUSIONS

We have introduced two new pair statistics, N_c and L_c , which are shown to be related to the galaxy merger and accretion rates respectively. Using Monte Carlo simulations, these statistics are found to be robust to the redshift-dependent density changes inherent in flux-limited samples; this represents a very significant improvement over all previous estimators. In addition, we provide a clear prescription for relating N_c and L_c to the galaxy CF and LF, enabling straightforward comparison with measurements on larger scales.

These statistics are applied to the SSRS2 survey, providing the first statistically sound measurements of pair statistics at low redshift. For an effective range in absolute magnitude of $-21 \leq M_B \leq -18$, we find $N_c = 0.0226 \pm 0.0052$ at $z=0.015$, implying that $\sim 2.3\%$ of these galaxies have companions within a projected physical separation of $5 h^{-1} \text{ kpc} \leq r_p \leq 20 h^{-1} \text{ kpc}$ and 500 km/s along the line of sight. If this pair statistic remains fixed with redshift, simple assumptions imply that $\sim 6.6\%$ of

present day galaxies with $-21 \leq M_B \leq -18$ have undergone mergers since $z=1$. For our luminosity statistic, we find $L_c = 0.0216 \pm 0.0055 \times 10^{10} h^2 L_\odot$. This statistic gives the mean luminosity in companions, per galaxy. Both of these statistics will serve as local benchmarks in ongoing and future studies aimed at detecting redshift evolution in the galaxy merger and accretion rates.

It is our hope that these techniques will be applied to a wide range of future redshift surveys. As we have demonstrated, one must carefully account for differences in sampling effects between pairs and field galaxies. This will be of increased importance when applying pair statistics at higher redshift, as k -corrections, luminosity evolution, band-shifting effects, and spectroscopic completeness have to be properly accounted for. The general approach outlined in this paper indicates the steps that must be taken to allow for a fair comparison between disparate surveys at low and high redshift. These techniques are applicable to redshift surveys with varying degrees of completeness, and are also adaptable to redshift surveys with additional photometric information, such as photometric redshifts, or even simply photometric identifications. Finally, this approach can be used for detailed studies of both major and minor mergers.

We wish to thank all members of the SSRS2 collaboration for their work in compiling the SSRS2 survey, and for making these data available in a timely manner. Digitized Sky Survey images used in this research were obtained from the Canadian Astronomical Data Centre (CADC), and are based on photographic data of the National Geographic Society Palomar Observatory Sky Survey (NGS-POSS). The Digitized Sky Surveys were produced at the Space Telescope Science Institute under U.S. Government grant NAG W-2166. This work was supported by the Natural Sciences and Engineering Research Council of Canada, through research grants to R.G.C. and C.J.P..

REFERENCES

- Alonso, M. V., da Costa, L. N., Pellegrini, P. S., & Kurtz, M. J. 1993, *AJ*, 106, 676
- Alonso, M. V., da Costa, L. N., Latham, D. W., Pellegrini, P. S., & Milone, A. E. 1994, *AJ*, 108, 1987
- Bahcall, S. R. & Tremaine, S. 1988, *ApJ*, 326, L1
- Barnes, J. E. 1988, *ApJ*, 331, 699
- Barnes, J. E. & Hernquist, L. 1992, *ARA&A*, 30, 705
- Barton, E. J., Bromley, B. C., & Geller, M. J. 1998, *ApJ*, 511, L25
- Benoist, C., Maurogordato, S., da Costa, L. N., Cappi, A., & Schaeffer, R. 1996, *ApJ*, 472, 452
- Binney, J., and Tremaine, S. 1987, in *Galactic Dynamics* (Princeton: Princeton University Press)
- Burkey, J. M., Keel, W. C., Windhorst, R. A., & Franklin, B. E. 1994, *ApJ*, 429, L13
- Carlberg, R. G., Pritchet, C. J., & Infante, L. 1994, *ApJ*, 435, 540
- Courteau, S., & van den Bergh, S. 1999, *AJ*, 118, 337
- da Costa, L. N., Willmer, C. N. A., Pellegrini, P. S., Chaves, O. L., Rit e, C., Maia, M. A. G., Geller, M. J., Latham, D. W., Kurtz, M. J., Huchra, J. P., Ramella, M., Fairall, A. P., Smith, C., & L ipari, S. 1998, *AJ*, 116, 1
- Davis, M., & Peebles, P. J. E. 1983, *ApJ*, 267, 465
- Dressler, A. 1980, *ApJ*, 236, 351
- Dubinski, J., Mihos, J. C., and Hernquist, L. 1999, *ApJ*, submitted
- Efron, B. 1981, *Biometrika*, 68, 589
- Efron, B., & Tibshirani, R. 1986, *Statistical Science*, 1, 54
- Ellis, R. S. 1997, *ARA&A*, 35, 389
- Hibbard, J. E., & van Gorkom, J. H. 1996, *AJ*, 111, 655
- Koo, D., & Kron, R. 1992, *ARA&A*, 30, 613
- Le F evre, O., Abraham, R., Lilly, S. J., Ellis, R. S., Brinchmann, J., Tresse, L., Colless, M., Crampton, D., Glazebrook, K., Hammer, F., & Broadhurst, T. 1999, *MNRAS*, In Press
- Lin, H., Yee, H. K. C., Carlberg, R. G., Morris, S. L., Sawicki, M., Patton, D. R., Wirth, G. D., & Shepherd, C. W. 1999, *ApJ*, 518, 533
- Loveday, J., Maddox, S. J., Efstathiou, G., & Peterson, B. A. 1995, *ApJ*, 442, 457
- Marzke, R. O., Geller, M. J., da Costa, L. N., & Huchra, J. P. 1995, *AJ*, 110, 477
- Marzke, R. O., da Costa, L. N., Pellegrini, P. S., Willmer, C. N. A., & Geller, M. J. 1998, *ApJ*, 503, 617
- Madau, P., Pozzetti, L., & Dickinson, M. 1998, *ApJ*, 498, 106
- Nilson, P. 1973, *Uppsala General Catalog of Galaxies* (Uppsala: Royal Society of Sciences of Uppsala)
- Patton, D. R., Pritchet, C. J., Yee, H. K. C., Ellingson, E., & Carlberg, R. G. 1997, *ApJ*, 475, 29
- Patton, D. R., Pritchet, C. J., Carlberg, R. G., Marzke, R. O., Yee, H. K. C., Ellingson, E., Hall, P. B., Lin, H., Morris, S. L., Sawicki, M., Schade, D., Shepherd, C. W., & Wirth, G. D. 2000, In Preparation
- Peebles, P. J. E. 1980, *The Large-Scale Structure of the Universe* (Princeton University Press: Princeton)
- Postman, M., & Geller, M. J. 1984, *ApJ*, 281, 95
- Toomre, A., & Toomre, J. 1972, *ApJ*, 179, 623
- Toomre, A. 1977, in *Evolution of Galaxies and Stellar Populations*, ed. B. M. Tinsley, & R. B. Larson (New Haven: Yale Obs.), p. 401
- Vogele, M. S. 1993, PhD Dissertation, Harvard University, Cambridge, MA USA
- Williams, R. E. et al. 1996, *AJ*, 112, 1335

Willmer, C. N. A., da Costa, L. N., Pellegrini, P. S. 1998, AJ, 115,
869
Woods, D., Fahlman, G. G., & Richer, H. B. 1995, ApJ, 454, 32

Yee, H. K. C., & Ellingson, E. 1995, ApJ, 445, 37
Zepf, S. E., & Koo, D. C. 1989, ApJ, 337, 34

TABLE 1

SSRS2 Pair Statistics

Sample	N	N_{comp}	\bar{z}	N_c	$L_c(10^{10}h^2L_\odot)$
SSRS2 North	1702	27	0.014	0.0189 ± 0.0074	0.0169 ± 0.0079
SSRS2 South	3067	53	0.016	0.0261 ± 0.0073	0.0262 ± 0.0078
SSRS2 (N+S)	4769	80	0.015	0.0226 ± 0.0052	0.0216 ± 0.0055

TABLE 2

SSRS2 North : Close Pairs and Triples

ID	N	r_p	Δv	RA(1950.0)	DEC(1950.0)	cz
1	2	17.3	75	11:18:00.6	-09:59:44	1523
2	2	12.7	385	12:23:39.7	-07:24:21	5183
3	2	19.8	392	12:39:42.8	-05:30:33	6604
4	2	18.1	357	12:49:52.3	-15:14:45	4539
5	2	13.0	183	12:50:31.4	-08:55:47	4149
6	3	11.4	42	13:01:21.2	-11:13:39	2965
7	2	12.3	227	13:17:00.1	-27:09:24	1835
8	2	6.5	198	13:23:14.6	-26:24:59	9596
9	2	18.1	99	13:30:31.8	-15:52:26	5813
10	2	12.5	70	13:32:37.2	-10:37:55	6550
11	2	15.7	298	13:57:36.5	-23:03:54	10592
12	2	12.8	4	14:01:52.3	-24:35:25	2117
13	2	17.4	90	14:10:41.5	-02:56:41	1664

TABLE 3

SSRS2 South : Close Pairs and Triples

ID	N	r_p	Δv	RA(1950.0)	DEC(1950.0)	cz
14	2	7.8	48	00:13:51.2	-06:35:57	8070
15	2	13.7	276	00:56:52.5	-05:04:07	5771
16	2	18.9	100	01:06:26.0	-28:51:25	5522
17	2	14.1	163	01:10:01.2	-04:24:30	5723
18	2	12.4	160	01:13:05.7	-06:51:23	6365
19	2	12.4	229	01:16:22.5	-17:04:00	6002
20	2	16.8	114	01:34:10.7	-37:35:09	5171
21	2	10.7	173	02:06:55.3	-10:22:13	4143
22	2	6.9	39	02:26:44.0	-11:03:15	4695
23	2	19.6	102	02:55:45.2	-10:33:21	4647
24	2	16.0	78	03:04:11.5	-39:13:15	6188
25	2	19.2	115	03:08:51.0	-09:06:01	4020
26	2	12.9	18	03:22:17.8	-03:12:17	2764
27	2	5.4	43	04:10:06.5	-32:59:21	1085
28	3	7.8	61	04:13:09.8	-28:36:32	5450
29	2	10.8	256	04:29:34.7	-29:51:29	4032
30	3	19.7	227	21:08:47.2	-23:22:03	10682
31	2	10.8	99	21:59:10.7	-32:13:26	2674
32	2	11.9	66	22:03:22.9	-28:11:55	7042
33	2	16.8	59	22:19:05.8	-25:50:09	6904
34	2	14.2	107	22:52:34.7	-34:09:30	8700
35	2	19.6	36	22:55:33.0	-04:02:30	3828
36	2	14.0	129	22:57:31.1	-13:05:22	3115
37	2	6.5	47	23:00:35.1	-09:15:38	7360
38	2	19.4	409	23:23:42.7	-39:29:48	10759
39	2	15.5	86	23:45:09.7	-28:24:56	8700

TABLE 4

SSRS2 Pair Statistics for Various Choices of $M_2(B)$

M_2	N_c	$L_c(10^{10}h^2L_\odot)$
-19.0	0.0082± 0.0019	0.0135± 0.0034
-18.9	0.0093± 0.0021	0.0144± 0.0037
-18.8	0.0105± 0.0024	0.0154± 0.0039
-18.7	0.0117± 0.0027	0.0163± 0.0042
-18.6	0.0131± 0.0030	0.0171± 0.0044
-18.5	0.0145± 0.0033	0.0180± 0.0046
-18.4	0.0159± 0.0037	0.0188± 0.0048
-18.3	0.0175± 0.0040	0.0195± 0.0050
-18.2	0.0191± 0.0044	0.0203± 0.0052
-18.1	0.0208± 0.0048	0.0210± 0.0054
-18.0	0.0226± 0.0052	0.0216± 0.0055
-17.9	0.0244± 0.0056	0.0222± 0.0057
-17.8	0.0263± 0.0060	0.0228± 0.0058
-17.7	0.0282± 0.0065	0.0234± 0.0060
-17.6	0.0302± 0.0070	0.0239± 0.0061
-17.5	0.0323± 0.0074	0.0244± 0.0062
-17.4	0.0344± 0.0079	0.0249± 0.0064
-17.3	0.0366± 0.0084	0.0253± 0.0065
-17.2	0.0388± 0.0089	0.0257± 0.0066
-17.1	0.0411± 0.0095	0.0261± 0.0067
-17.0	0.0435± 0.0100	0.0264± 0.0068

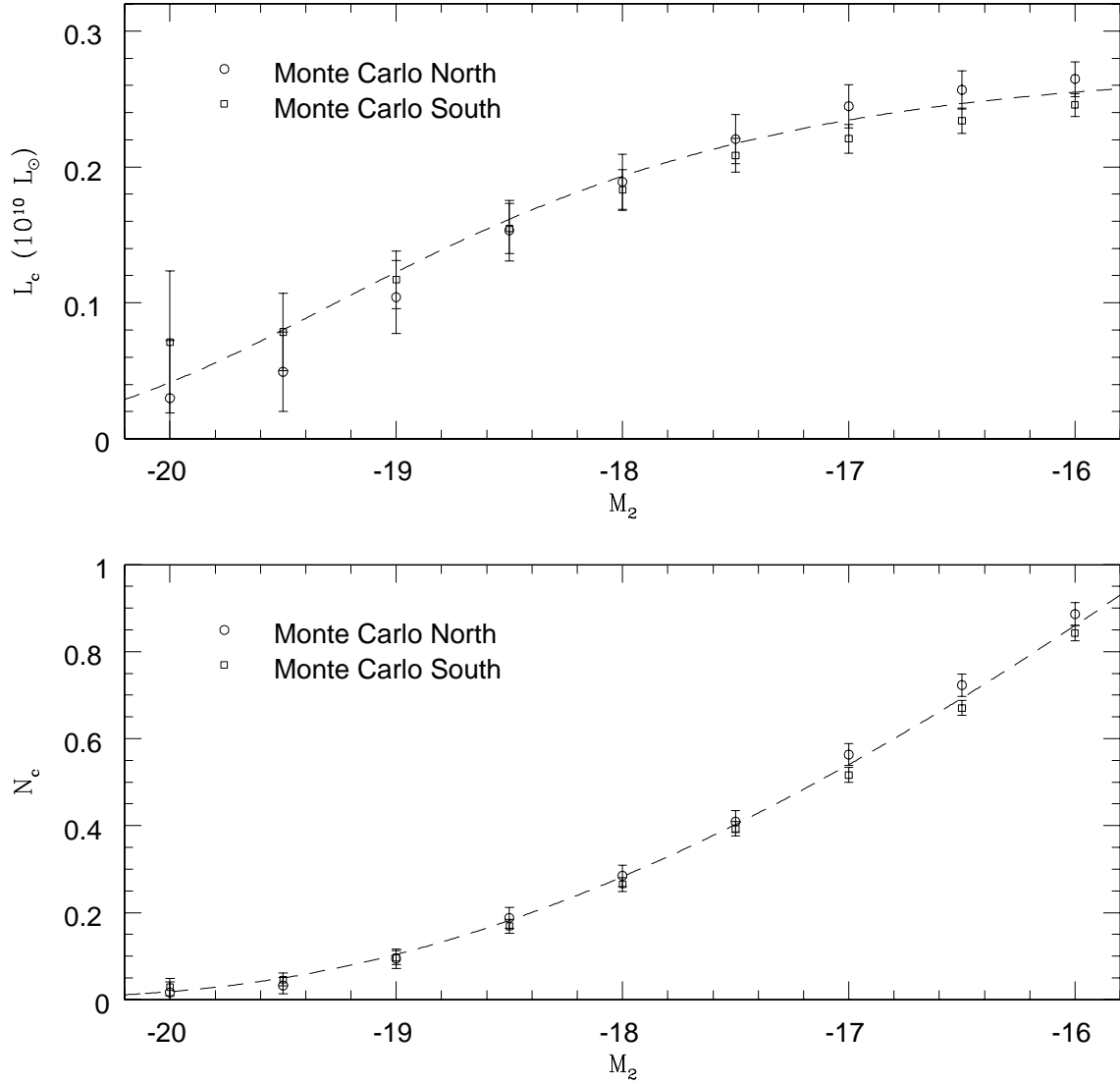


FIG. 1.— Pair statistics are computed for the volume-limited Monte Carlo simulations. N_c and L_c are given for a range of choices of M_2 , with $M_1=M_2$. Error bars are computed using the Jackknife technique. The dashed lines are the relations predicted using the input SSRS2 luminosity function, and normalized to match the data at $M_2=-16$.

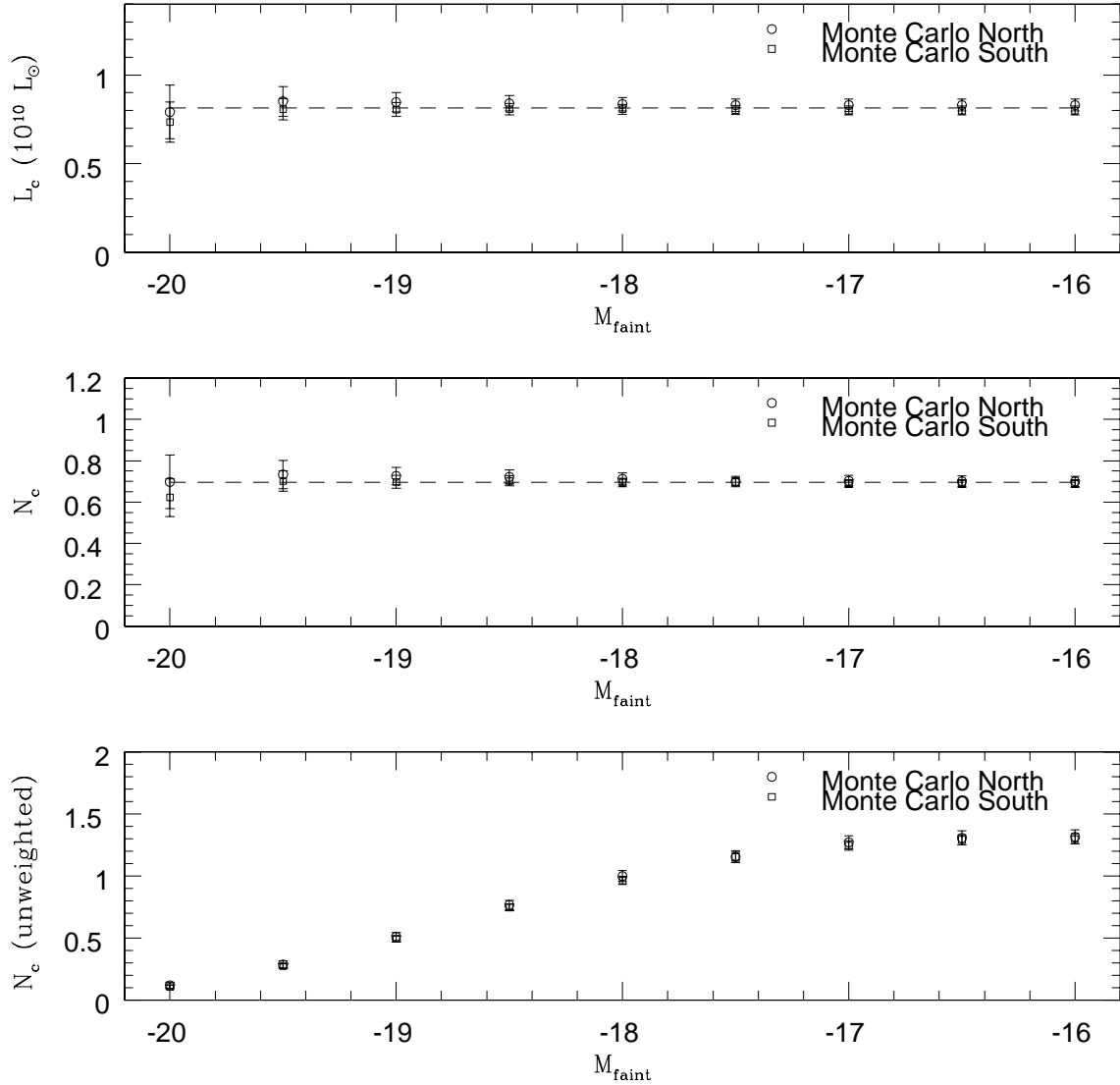


FIG. 2.— Pair statistics are computed for the flux-limited Monte Carlo simulations. Three pair statistics (unweighted N_c , N_c , and L_c) are given, for a range of choices of minimum luminosity M_{faint} , with $M_2=M_1=-19$. Error bars are computed using the Jackknife technique. The unweighted N_c exhibits a systematic increase with M_{faint} . This is a consequence of not correcting for the corresponding increase in mean galaxy number density. This bias is taken into account when computing N_c and L_c . The horizontal dashed lines match the data at $M_{\text{faint}}=-16$, and demonstrate that N_c and L_c do not depend on M_{faint} .

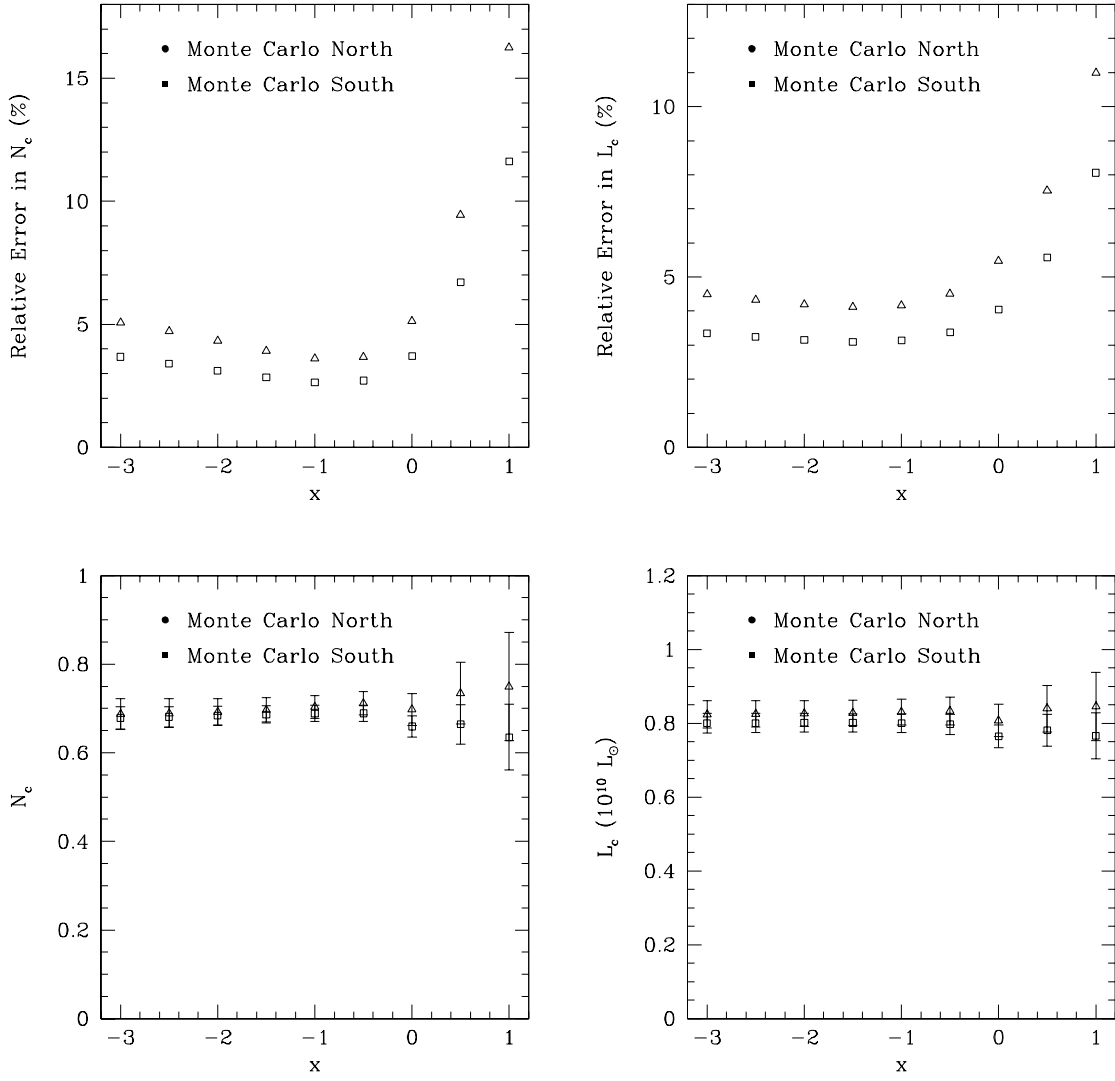


FIG. 3.— Pair statistics are computed for a range of possible weighting schemes for primary galaxies. Error bars are computed using the Jackknife technique.

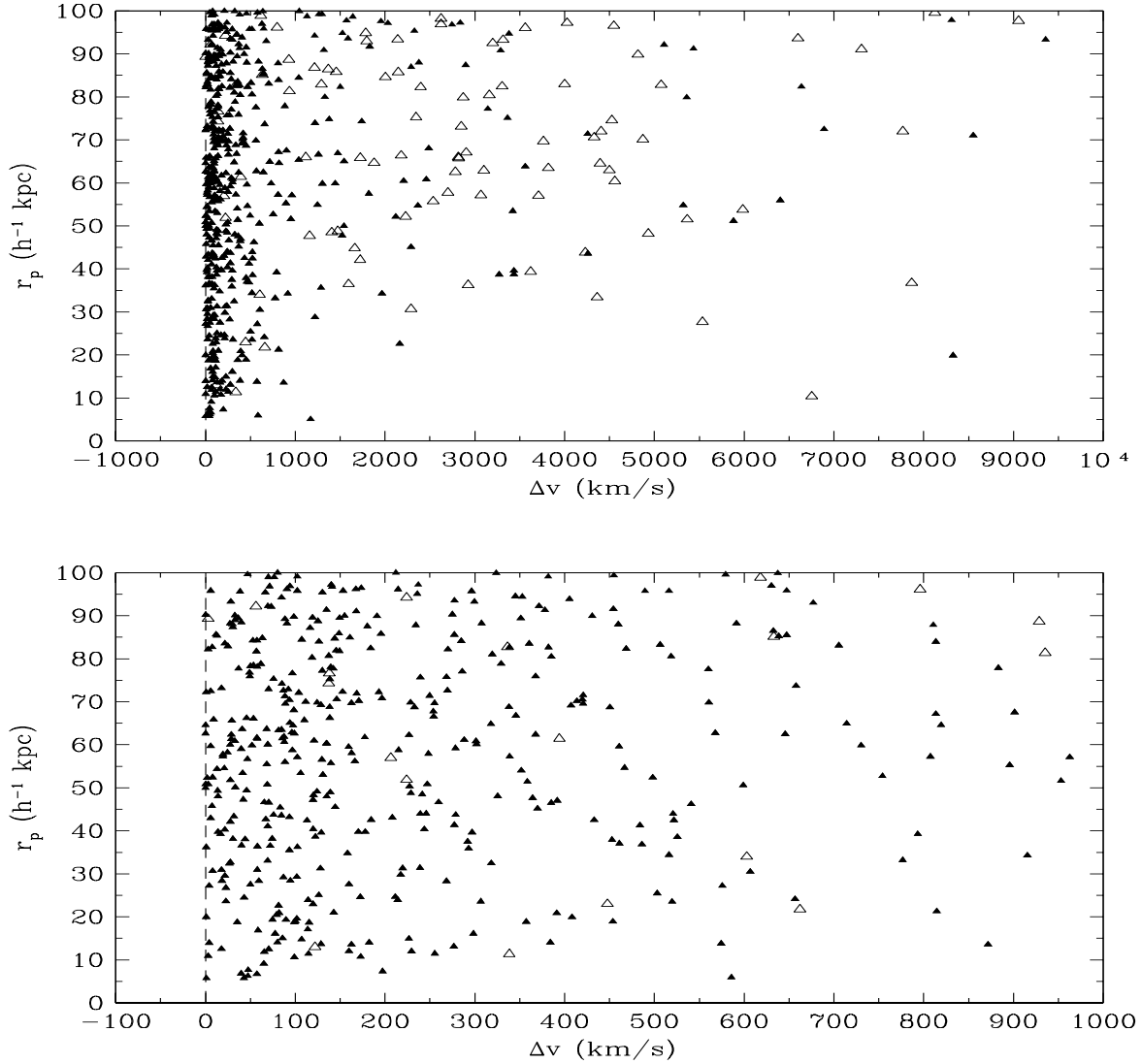


FIG. 4.— Projected separation (r_p) is plotted versus rest-frame velocity difference (Δv) for all pairs with $r_p \leq 100 h^{-1}$ kpc. Pairs were identified by looking for close companions (real or random) around primary galaxies in the SSRS2 survey. Filled triangles represent real companions found in the SSRS2 survey. Open triangles denote random companions found in the Monte Carlo simulations. Note that the density of the simulations was matched to the real data sample when generating this plot, ensuring a fair comparison. The upper plot gives a wide range in velocity differences, demonstrating how the number of companions in excess of random becomes negligible beyond ~ 1000 km/s. The lower plot is a zoomed-in version of the upper plot, giving a better feel for the distribution of physical pairs.

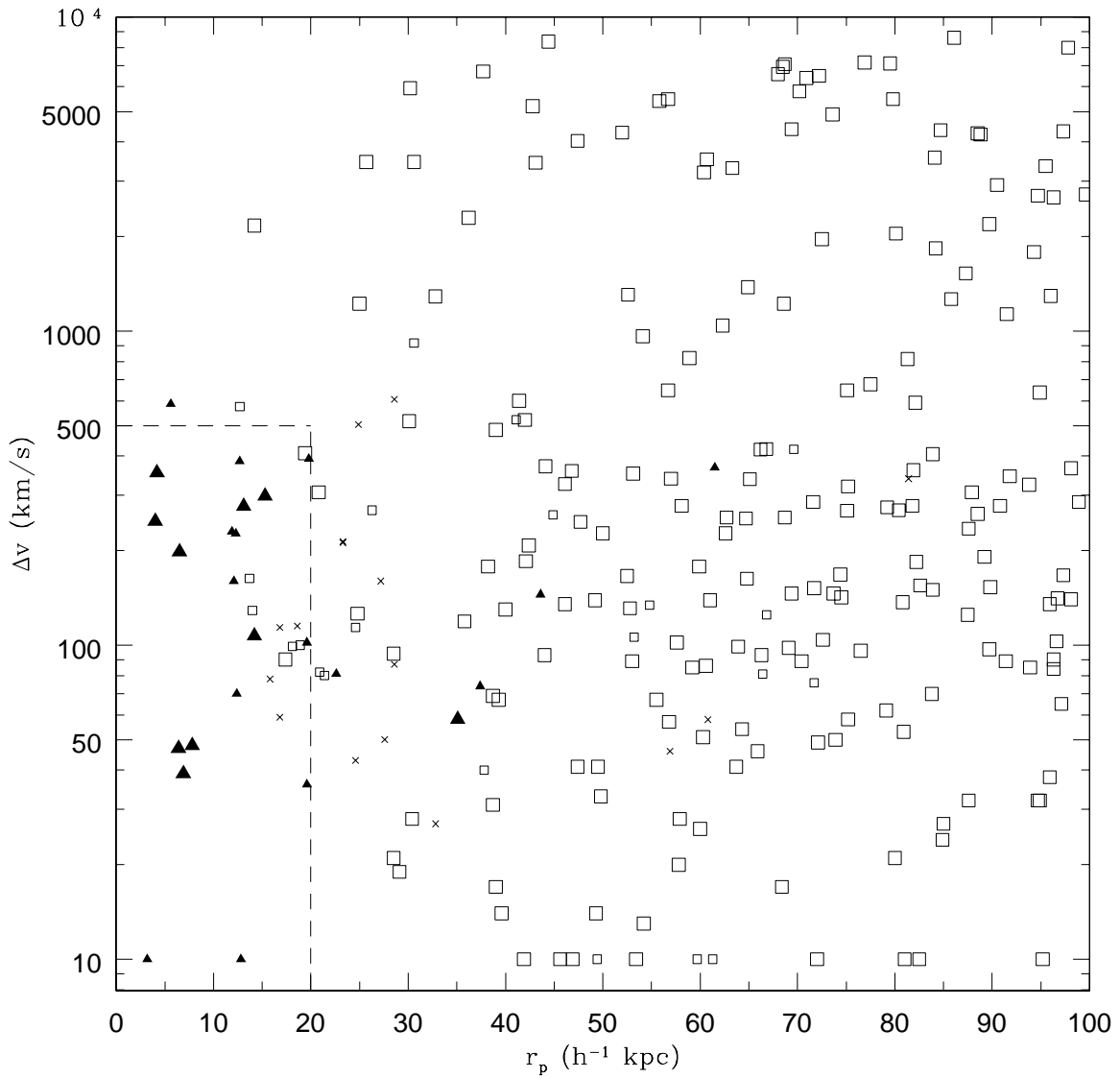


FIG. 5.— Pair interaction classification (I_c) is plotted as a function of projected physical separation (r_p) and line-of-sight rest-frame velocity difference (Δv), for 255 unique SSRS2 pairs with $r_p < 100 h^{-1}$ kpc. Symbols are defined as follows : $I_c=0,1$ (large open squares), $I_c=2,3$ (small open squares), $I_c=4-6$ (crosses), $I_c=7,8$ (small filled triangles), and $I_c=9,10$ (large filled triangles). High I_c indicates increased likelihood of interaction. For plotting convenience, pairs with $\Delta v < 10$ km/s are assigned $\Delta v = 10$ km/s. The dashed line marks the close pair criteria ($r_p=20 h^{-1}$ kpc and $\Delta v=500$ km/s) used for computing pair statistics.

See f6a.gif, f6b.gif, f6c.gif

FIG. 6.— A mosaic of images is given for the 38 close ($5 h^{-1}$ kpc $< r_p \leq 20 h^{-1}$ kpc) dynamical ($\Delta V < 500$ km/s) pairs or triples satisfying the criteria used for computing pair statistics. These images were obtained from the Digitized Sky Survey. Each image is $50 h^{-1}$ kpc on a side, corresponding to angular sizes of $1.5'-10'$.

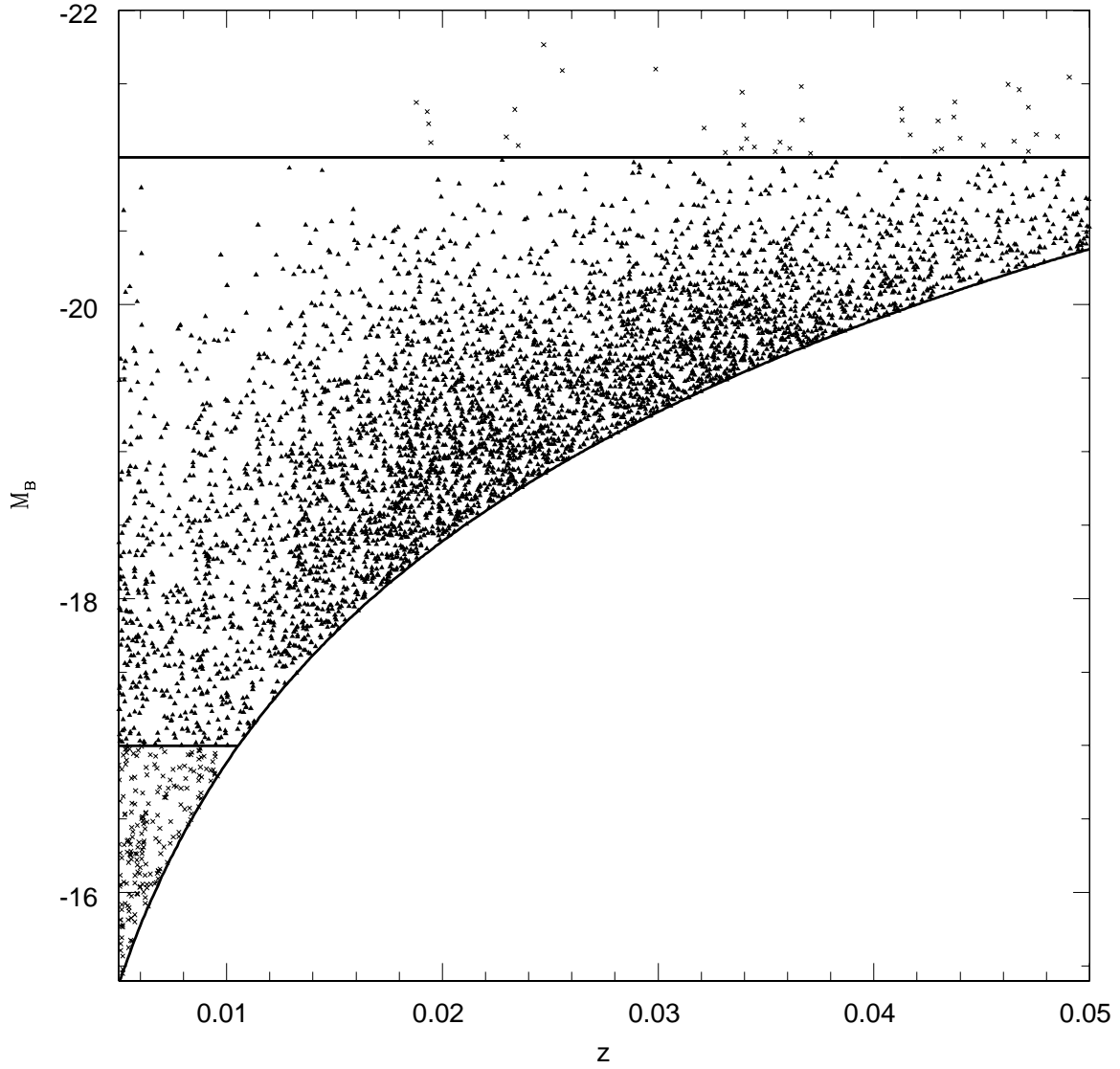


FIG. 7.— B -band absolute magnitude is plotted versus redshift for all SSRS2 galaxies with $m_B \leq 15.5$ and $0.005 \leq z \leq 0.05$. The curved line marks the boundary imposed by this apparent magnitude limit. The upper horizontal line indicates the bright limit imposed ($M_{\text{bright}} = -21$), while the lower horizontal line denotes the minimum luminosity allowed ($M_{\text{faint}} = -17$). Galaxies satisfying all of these criteria (and hence used in the calculation of N_c and L_c) are marked with triangles; the remainder are indicated with crosses.

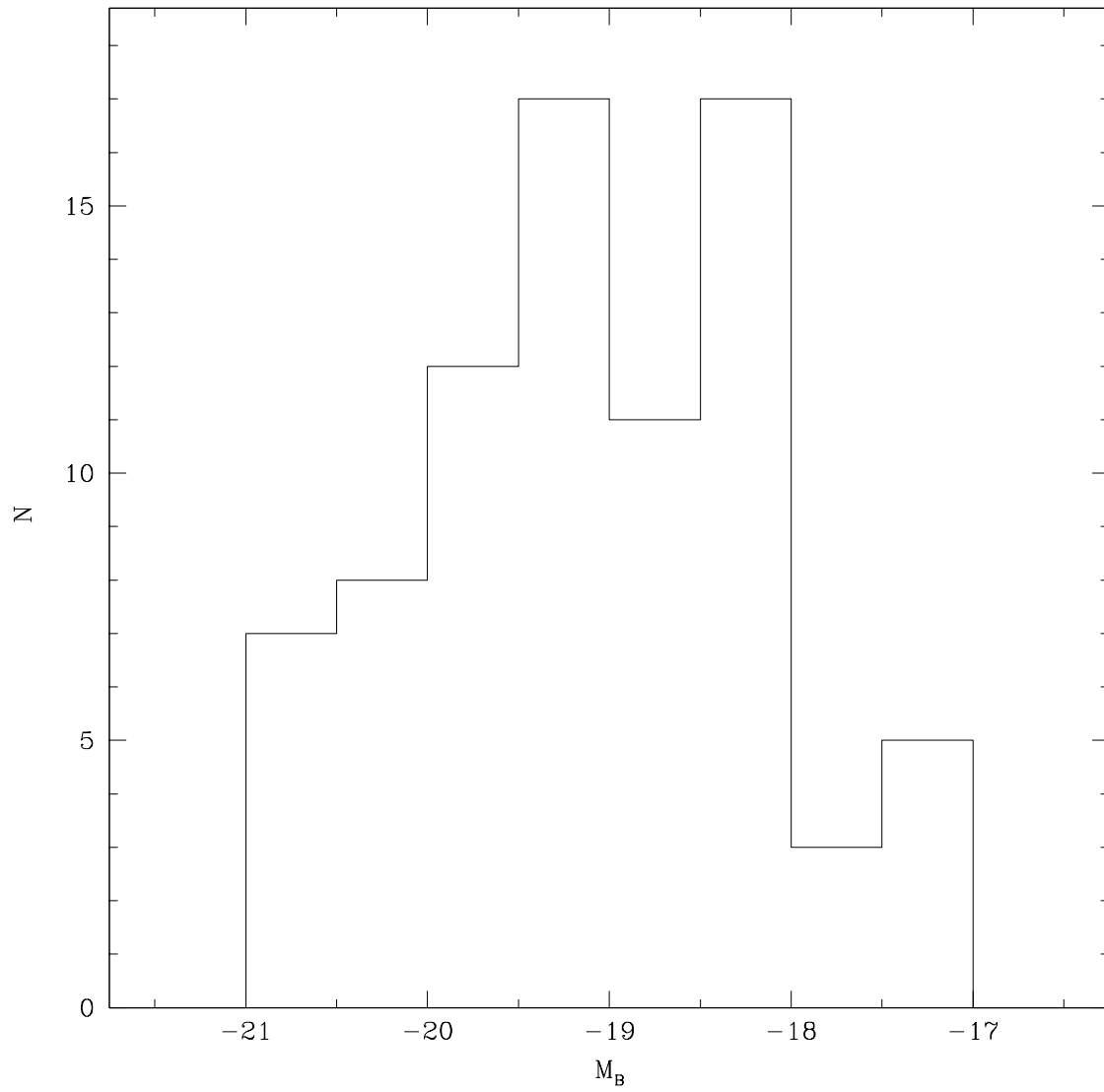


FIG. 8.— An absolute magnitude histogram is given for the 80 companions used in the pair statistics.

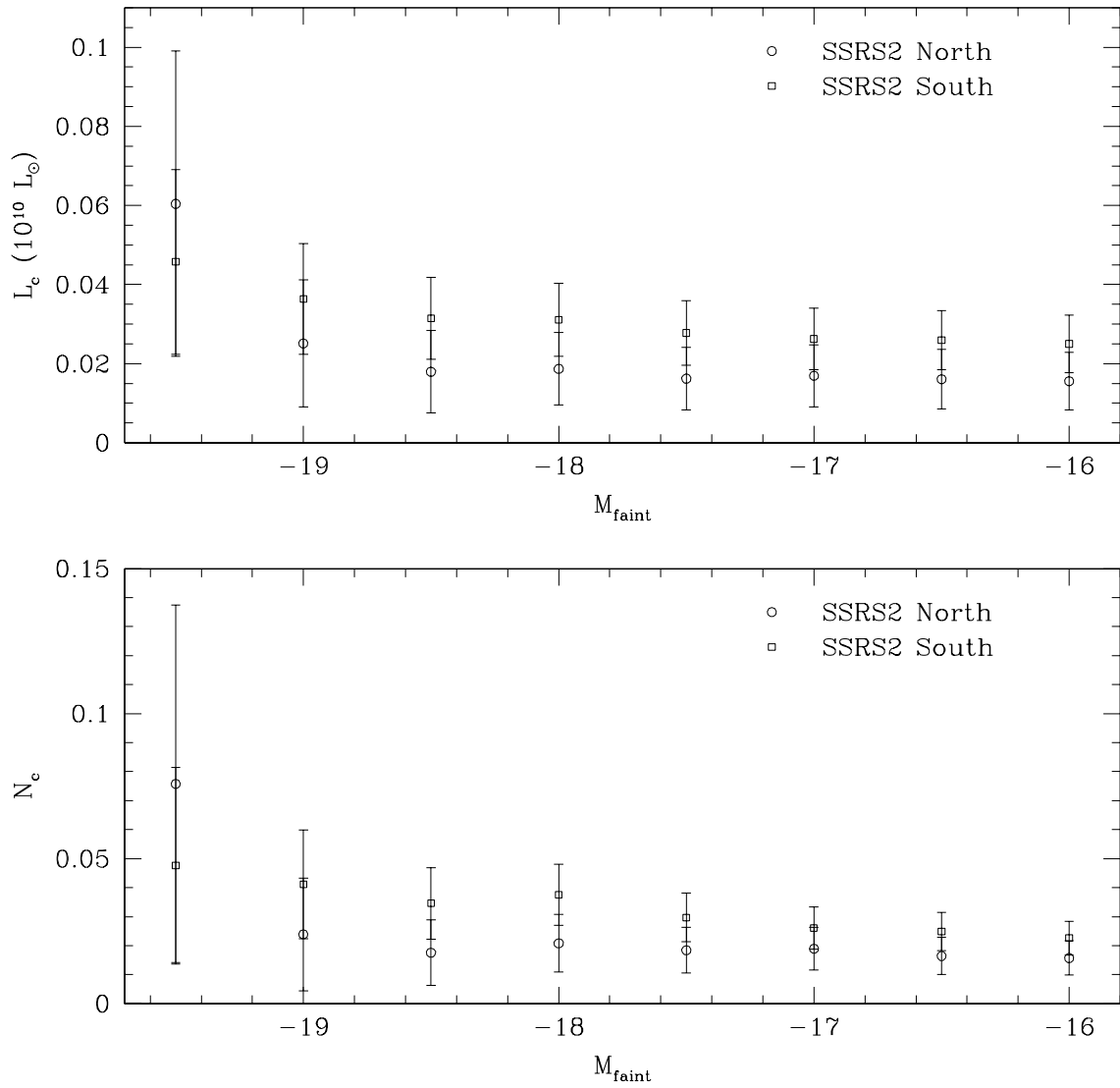


FIG. 9.— Pair statistics are computed for SSRS2 North and South. N_c and L_c are given, for a range in minimum luminosity M_{faint} , with $M_2=M_1=-18$. Error bars are computed using the Jackknife technique. Both N_c and L_c appear to be independent of M_{faint} , within the errors, over the range $-18 \leq M_{\text{faint}} \leq -16$. This implies that, to first order, clustering is independent of luminosity in this regime.

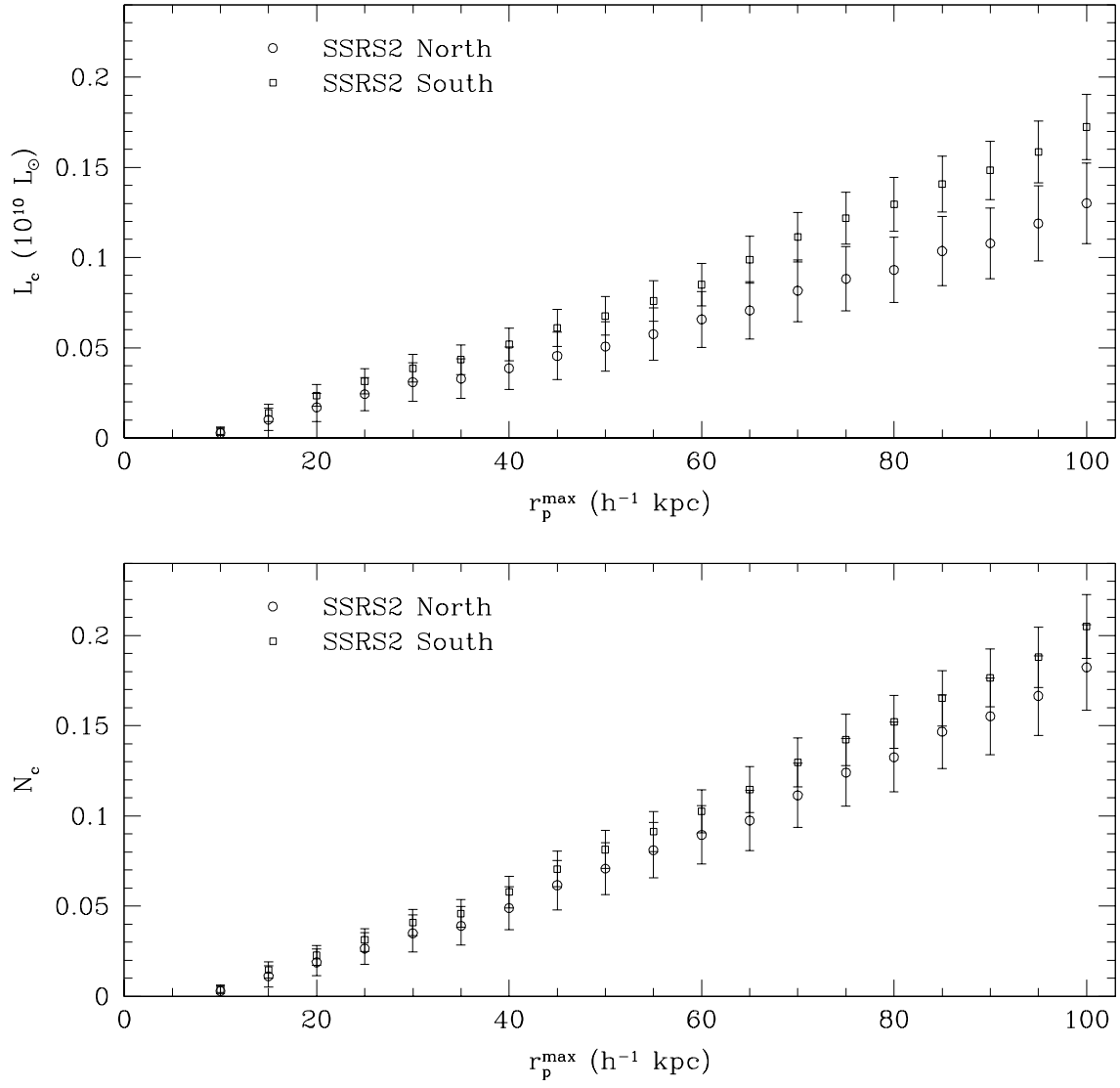


FIG. 10.— Pair statistics are computed for $\Delta v \leq 500$ km/s, for a range of maximum projected separations (r_p^{\max}). A minimum projected separation of $r_p = 5 h^{-1}$ kpc is applied in each case. Error bars are computed using the Jackknife technique. Both N_C and L_C are cumulative statistics; hence, measurements in successive bins are not independent.

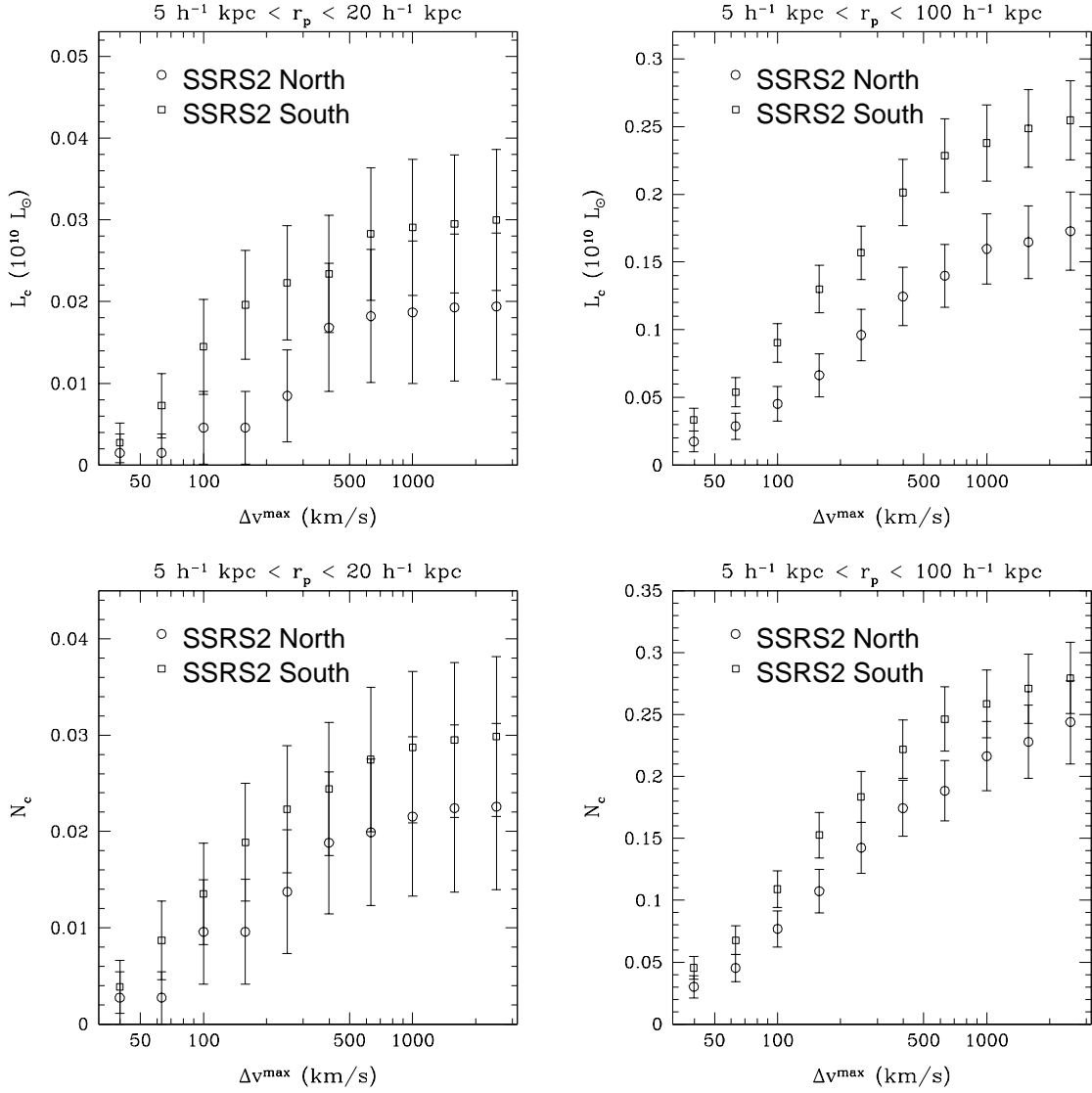


FIG. 11.— Pair statistics are computed for $\Delta v \leq 500$ km/s, for a range of projected separations. Error bars are computed using the Jackknife technique. Both N_c and L_c are cumulative statistics; hence, measurements in successive bins are not independent.

This figure "f6a.gif" is available in "gif" format from:

<http://arxiv.org/ps/astro-ph/0001364v2>

This figure "f6b.gif" is available in "gif" format from:

<http://arxiv.org/ps/astro-ph/0001364v2>

This figure "f6c.gif" is available in "gif" format from:

<http://arxiv.org/ps/astro-ph/0001364v2>